Coordination Chemistry Reviews 254 (2010) 916–937

Contents lists available at ScienceDirect

Coordination Chemistry Reviews

journal homepage: www.elsevier.com/locate/ccr

Review

Alcohol dehydrogenase and its simple inorganic models

Anna Dołęga*

Gdańsk University of Technology, Department of Inorganic Chemistry, Narutowicza St. 11/12 80-233, Gdańsk, Poland

Contents

ARTICLE INFO

Article history:
Received 2 November 2009
Accepted 29 December 2009
Available online 11 January 2010

ABSTRACT

Despite the long and extensive research, the mechanism of action of zinc-dependent alcohol dehydrogenase on the molecular level is still uncertain. The present state of knowledge of the mechanism of catalytic action of the alcohol dehydrogenase is presented, with the emphasis on the organization of the active site. The other part of the review is devoted to the description of model complexes with particular

Abbreviations: ADH, alcohol dehydrogenase; FDH, formaldehyde dehydrogenase; LADH, liver alcohol dehydrogenase; MDR, medium-chain dehydrogenases/reductases; NAD^+/NADH, nicotinamide adenine dinucleotide oxidized/reduced; [12]aneN$_3$, 1,5,9-triazacyclododecane; benpa, (*N*,*N*-bis-2-(ethylthio)ethyl-*N*-(6-neopentylamino-2-pyridylmethyl)amine); bmapa, *N*,*N*-bis-2-(methylthio)ethyl-*N*-(6-amino-2-pyridylmethyl)amine); bmnpa, *N*-bis-2-(methylthio)ethyl-*N*-(6-neopentylamino-2-pyridylmethyl)amine; bmpa, *N*,*N*-bis-2-(methylthio)ethyl-*N*-(2-pyridylmethyl)amine); BNA^+/BNA(Cl)/BNAH, nicotinamide benzyl chloride oxidized/oxidized/reduced; Bp^{Me}, bis(3,5-dimethylpyrazol-2-yl)diphenylmethanol; bpy, bipyridine; Calix[6]N$_3$ArO, 5,11,17,23,29,35-Hexa-*tert*-butyl-37,39,41-trimethoxy-38-[2-[(3,5-di-*tert*-butyl-2-hydroxy)benzyl]-amino]-ethoxy]-40,42-bis[(1-methyl-2-imidazolyl)methoxy]calix[6]arene; CO_2Et, 3-carboxyethyl; Cum, cumenyl; DMEP, 2,6-di-[(2′2′-diphenyl-2′-mercapto)ethyl]pyridine; ebnpa, *N*-2-(ethylthio)ethyl-*N*,*N*-bis(6-neopentylamino-2-pyridylmethyl)amine; 2-EtIm, 2-ethylimidazole; HB(mim$^{o\text{-}An}$)$_2$(pz^{Ph,Me}), bis[1-(*o*-anisyl)mercaptoimidazolyl][(3-phenyl-5-methyl)pyrazolyl]hydroborate; H$_2$MIEH, mercaptoisobuthyl-hydroxyethylamine; $L_{S2(Me)N3(Pr)}$, 1,2-dimethyl-3,7,1-triazatrideca-2,11-diene-1,13-dithiol; 2-MeIm, 2-methylimidazole; Mes, mesityl; MesCHO, mesitylaldehyde; *o*-An, *o*-anisyl; pbnpa, *N*-2-(phenylthio)ethyl-*N*,*N*-bis-((6-neopentylamino-2-pyridyl)methyl)amine; phen, phenantroline; Pic, 5′-picolyl; PicCHO, 2-methylpyridine-6-carbaldehyde; PicMeOH, 6-hydroxymethyl-2-methylpyridine; *p*-Tol, *para*-tolyl; Py, 4′-pirydyl; PyCHO, pyridine-2-carbaldehyde; *t*BuA, *tert*-butylcarboxamido; Tm^{Mes}, tris[1-(mesityl)-2-mercaptoimidazolyl]hydroborate; Tm^{Tol}, tris[1-(*p*-tolil)-2-mercaptoimidazolyl]hydroborate; $Tm^{2,6\text{-}Xy}$, tris[1-(2′,6′-xylil)-2-mercaptoimidazolyl]hydroborate; $Tp^{CO2Et,Me}$, tris[(3-carboxyethyl-5-methyl)pyrazolyl]hydroborate; $Tp^{Cum,Me}$, tris[(3-*p*-cumenyl-5-methyl)pyrazolyl]hydroborate; $Tp^{Pic,Me}$, tris[(3-(5′-picolyl)-5-methyl)pyrazolyl]hydroborate; $Tp^{tBuA,Me}$, tris[(3-*tert*-butylcarboxamido-5-methyl)pyrazolyl]hydroborate; $Tp^{tBu,Me}$, tris[(3-*tert*-butyl-5-methyl)pyrazolyl]hydroborate; TriMim, 1,3,5-triethyl-2,4,6-tris[N-methyl-imidazole-2-yl-thiomethyl]benzene; X$_6$Et$_3$Imet$_3$, 5,11,17,23,29,35-Hexa-*tert*-butyl-37,39,41-trimethoxy-38,40,42-tris[(1-methyl-2-imidazolyl)methoxy]calix[6]arene; 2,6-Xy, 2,6-xylil.

* Tel.: +48 58 347 23 51; fax: +48 58 347 26 94.
E-mail address: ania@chem.pg.gda.pl.

0010-8545/$ – see front matter © 2010 Elsevier B.V. All rights reserved.
doi:10.1016/j.ccr.2009.12.039

Keywords:
Alcohol dehydrogenase
Mechanism of action
Structure
Model complexes
Thiolates

attention paid to the structural aspect of model studies. Attempts to create an artificial system exhibiting dehydrogenase activity are also described.

© 2010 Elsevier B.V. All rights reserved.

1. Introduction

Catalytic and structural zinc sites are present in hundreds of enzymes and thousands of zinc finger DNA-binding protein domains. They all contain zinc ion complexed by nitrogen, oxygen, and sulfur ligands from the side chains of histidine, glutamate/aspartate, and cysteine, respectively [1]. Different coordination environments formed by the amino acid ligands influence the chemical characteristics of zinc which allows this element to be either metabolically active or inert [2]. Catalytic zinc atoms are complexed by three amino acid side chains, whereas structural zinc is bonded to four protein ligands. Histidine is the most frequent amino acid in catalytic sites while cysteine is most frequent in the structural ones [3]. The presence of the water molecule as the fourth ligand to zinc is a universal feature of all catalytic zinc sites. The water is either activated by the zinc ion or displaced during the catalytic cycle [4]. A qualitative characterization of the coordination environments of catalytically active zinc sites is presented in Table 1 [5]. The structures and functions of zinc-dependent enzymes were reviewed in 2004 [6]. The structural features of zinc-binding sites in proteins were characterized [1,3,4,7,8], moreover attempts to identify the zinc-binding motifs on the basis of the physicochemical environment around the zinc in a protein have recently been undertaken [9].

The abundance of protein zinc sites together with the simplicity of synthesis of the zinc complexes caused enormous interest of the scientific community in the coordination chemistry of zinc. A search in Cambridge Structural Database (CSD), conducted at the end of 2009, revealed almost 13,000 structures of zinc complexes with various proportions of sulfur, oxygen and nitrogen ligands [10]. A considerable amount of work has been done to model zinc coordination environments in proteins. An exhaustive review by Parkin was devoted to this very aspect of coordination chemistry of zinc [11]. The other reviews on the subject of model complexes, but with a more restricted scope were those of Vahrenkamp [12] describing zinc complexes with pyrazolylborate ligands, Otero et al. [13] covering syntheses and coordination chemistry of heteroscorpionate ligands based on bis(pyrazol-1-yl)methane, and Parkin [14] again discussing synthetic analogues of zinc enzymes based on tripodal ligands. In 2005 Weston published a review on the mode of action of bi- and trinuclear zinc hydrolases and their synthetic analogues [15]. Three years ago Berreau described the bioinorganic aspect of chemistry of synthetic zinc complexes supported by tripodal tetradentate chelate ligands containing internal hydrogen bond donors [16]. The following year the same author published an overview on coordination and bioinorganic chemistry of aryl-appended tris(2-pirydylmethyl)amine ligands [17]. Organometallic and bioinorganic aspects of the chemistry of zinc, cadmium and mercury in sulfur- and selenium-rich coordination environments provided by the tripodal tris(2-mercapto-1-R-imidazolyl) hydroborato ligands and their selenium analogues were discussed by Parkin in 2007 [18]. Most recently, in 2009, research on biomimetic calix[6]arene-based receptors for neutral molecules was summarized by Reinaud and co-workers [19].

Following Weston's approach, this review covers simple inorganic models of the active site of horse-liver form of alcohol dehydrogenase (LADH) regardless of the choice of ligands present in the structure of the zinc complex. The first part of the review contains the present state of knowledge about the mechanism of catalytic action of the alcohol dehydrogenase with the emphasis on the organization of the active site. The second part is devoted to the description of model complexes with particular attention paid to the structural aspect of model studies. Finally, attempts to model the function of LADH are described. With only few exceptions, the review does not encompass the theoretical studies on LADH models.

2. Protein

2.1. Function of liver alcohol dehydrogenase LADH

The alcohol dehydrogenase (ADH) family consists of several enzymes able to catalyze the reversible oxidation of a wide variety of primary and secondary alcohols to the corresponding aldehydes and ketones [20]. Functional roles of ADHs are not fully understood. Based on their catalytic activities, ADHs are supposed to participate in the metabolism of steroids, retinoids, lipid peroxidation products, ω-hydroxy fatty acids as well as xenobiotic alcohols and aldehydes. ADH3 (or formaldehyde dehydrogenase FDH) which is an ancestral form, is the only member of the family that has been ascribed a physiological substrate, i.e. S-hydroxymethylglutathione, and is identified as a functional formaldehyde scavenger. Its widespread occurrence and conserved structure imply the essential functions in living organisms [21,22]. ADH1 is the major enzyme in the metabolism of ingested ethanol [21], while ADH4 is the one involved in the first-pass metabolism of ethanol in stomach [23].

The ADH system can be regarded as a major detoxifying machinery for alcohols and aldehydes. The conversion of ethanol to acetaldehyde coupled with the reduction of NAD^+ to NADH results in an altered NAD/NADH ratio and is responsible for many metabolic effects of ethanol [24]:

$$CH_3CH_2OH + NAD^+ = CH_3CHO + NADH + H^+$$

A smaller part (~10%) of the ingested alcohol is metabolized by different pathways, mainly by cytochrome P450 isoform CYP2E1 [24,25]:

$$CH_3CH_2OH + NADPH + H^+ + O_2 = CH_3CHO + NADP^+ + 2H_2O$$

2.2. Structure and mechanism of action of LADH

Liver alcohol dehydrogenase belongs to the large superfamily of medium-chain dehydrogenases/reductases MDRs which now encompasses almost 11,000 members [23,26,27]. The MDR proteins consist of two domains, i.e. the C-terminal domain which contains coenzyme-binding Rossmann fold and the N-terminal domain responsible for substrate binding. The domains are separated by a cleft with a deep pocket which brings the cofactor and the active site in contact [27]. Until 1999, seven classes of vertebrate ADHs (EC 1.1.1.1) were recognized based upon sequence alignment, catalytic properties and some other features [20]. However, the major forms of mammalian enzymes are dimeric, with a subunit molecular mass of 40 kDa and two tightly bound zinc ions per sub-

Table 1
Coordination of zinc in mononuclear catalytic sites [5].

The number of S atoms	The number of N atoms	Coordination pattern	*Example* of protein/function/remarks	Reference	RCSB PDB symbol[a]
0	2	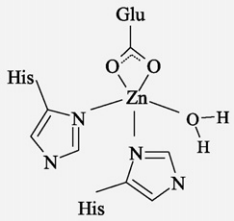	*Bovine* carboxypeptidase A/hydrolysis of the peptide bonds—exopeptidase and exoesterase	[5a]	1M4L
			Bacillus thermoproteolyticus thermolysin/an endopeptidase specific for peptide bonds on the imino side of hydrophobic residues	[5b]	1FJV
0	3	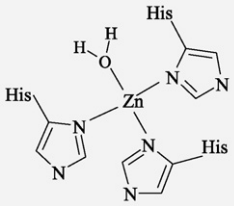	*Human* carbonic anhydrase II/catalysis of the hydration of carbon dioxide and dehydration of bicarbonate	[5c]	1TEQ
			Human matrix metalloproteinase-1 (fibroblast collagenase) degradation of interstitial collagen—peptidase	[5d]	2CLT
1	1	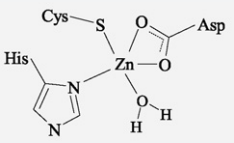	*Rat* FTase/the carboxyl-terminal lipidation of Ras and several other cellular signal transduction proteins	[5e]	1FT1
1	1	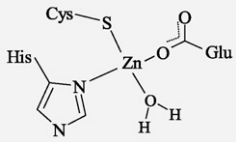	*S. cerevisiae* PI-SceI endonuclease/transesterification and succinimide formation (protein splicing)	[5f]	1VDE
			Aeropyrum pernix Alcohol dehydrogenase/dehydrogenation of primary and secondary alcohols/Asp instead of Glu	[5g]	1H2B
1	2	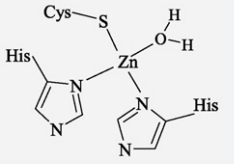	*Bacteriophage T7* lysosyme/probably—cleavage of amide bonds (amidase)	[5h]	1LBA
1	3	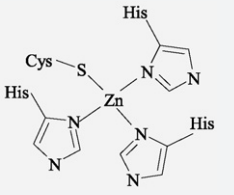	*Human* proMMP-1/blocked hydrolase—proenzyme	[5i]	1SU3
2	1	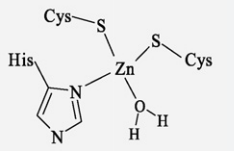	*Human* alcohol dehydrogenase/dehydrogenation of primary and secondary alcohols	[5j]	1HSZ
			E. coli cytidine deaminase/hydrolytic deamination of cytidine to uridine	[5k]	1CTT
			Human GTP cyclohydrolase I/catalyzes the conversion of GTP to dihydroneopterin triphosphate	[5l]	1FBX
3	0	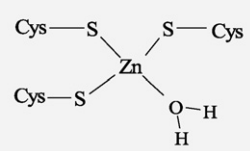	*Yeast* 5-aminolaevulinic acid dehydratase/second step in the biosynthesis of tetrapyrroles—condensation of two molecules of 5-aminolaevulinic acid with the formation of asymmetric pyrrole	[5m]	1H7N

[a] RCSB PDB symbol = the symbol of the entry in the Protein Data Bank managed by the Research Collaboratory for Structural Bioinformatics http://pdb.rcsb.org/pdb/home/home.do.

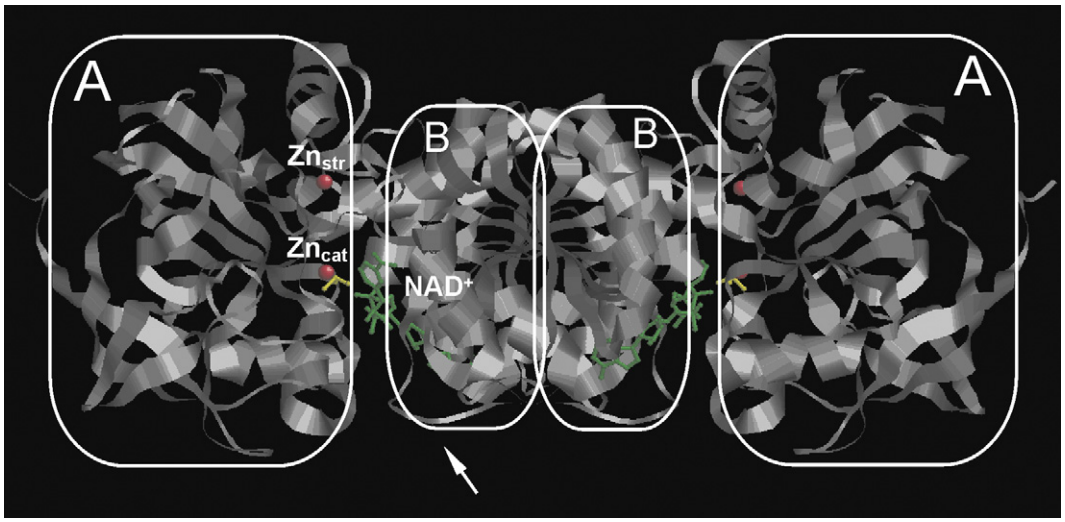

Fig. 1. Two domains: a catalytic domain (A) and a coenzyme-binding domain (B) form a subunit of the LADH dimer. Catalytic and structural zincs (pink) are indicated in the catalytic domain, and NAD^+ (green) in the coenzyme-binding domain. The arrow points at the substrate entrance. The figure was prepared from the RCSB PDB entry 2OHX [29] with the program RasMol.

unit [28].[1] Each subunit of the dimeric enzyme has two domains, i.e. the catalytic domain and the coenzyme-binding domain. The catalytic domain is larger and contains substrate-binding zinc ion as well as all the amino acid residues which participate in the catalyzed reaction. The two coenzyme-binding domains form a central core of the LADH dimer (Fig. 1 [29]) [28,30].

The mechanism of action of LADH includes the following steps:

- NAD^+ binding and closing of the catalytic site by the domain rotation;
- binding of alcohol (i.e. a substrate) to the catalytic zinc ion with the parallel displacement of the water molecule;
- dissociation and transportation of proton from the hydroxyl group of an alcohol out of the catalytic site *via* the hydrogen bond network;
- hydride transfer from the zinc-bound alcoholate to the nicotinamide ring;
- aldehyde departure and replacement by a neutral water molecule;
- opening of the catalytic site accompanied by the release of NADH [23,28].

The steps listed above may be summarized by one of the following equations:

$$R_1R_2CHOH + NAD^+ = R_1R_2CO + NADH + H^+$$

or

$$R_1R_2CHOH + NAD^+ + H_2O = R_1R_2CO + NADH + H_3O^+$$

2.2.1. NAD^+ binding and closing of the catalytic site by the domain rotation

An obligatory binding order of the coenzyme followed by the substrate was established by Theorell and Chance nearly 60 years ago [31]. In 1973 in their first paper concerning the crystal structure of LADH Brånden and co-workers [32] described a coenzyme-binding substructure consisting of about 120 amino acids in each subunit of LADH. The researchers pointed out to the similarity between the conformation of this substructure and the corresponding coenzyme-binding parts of two other dehydrogenases. This protein structural motif possessing beta/alpha/beta folds is presently known as Rossmann fold [33]; each LADH coenzyme-binding subunit consists of two such folds (one for each nucleotide in NAD^+). A joint system of hydrophobic interactions and hydrogen bonds that maintains coenzyme position includes over 20 amino acid residues [34]. The position of NAD^+ within a ternary complex with LADH is presented in Fig. 2. The adenine base is placed in a hydrophobic cleft with the amino group at position 6 pointing out towards the protein surface, thus it is the only part of the coenzyme exposed to solvent. The adenosine ribose is bound with hydrogen bonds to the side chains of aspartate (Asp-223) and lysine (Lys-228). Pyrophosphate of NAD^+ is attached with hydrogen bonds to the main peptide chain *via* two arginine residues, i.e. Arg-47 and Arg-369 (the latter is not shown in Fig. 2). Nicotinamide ribose is hydrogen bonded to the main chain carbonyl *via* Ser-48 and His-51 [35]. Nicotinamide interacts with the main chain *via* hydrogen bonds formed by its amino group. It is also precisely positioned in the vicinity of the active site as a result of the hydrophobic interactions with the side chains of Val-203, Val-292, and Thr-178 (the first one is shown in Fig. 2) which remain in contact with the unreactive face of the ring. The other face of the ring is directed towards the active site close to the catalytic zinc ion [35–38].

Binding of the coenzyme is accompanied by a large conformational change of the protein. Alcohol dehydrogenase was the first enzyme for which domain rotations were demonstrated [35,39]. In the apoenzyme[2] structure the central cleft is accessible to solvent and ligands, whereas in the holoenzyme the cleft is closed off by the relative motion of the domains. The catalytic domain of LADH rotates by 10° in order to go from the apoenzyme to the holoenzyme structure [34,40]. As a result of the motion, residual water is expelled from the catalytic site and a hydrophobic environment needed for the hydride transfer is achieved. The conformational change induced by coenzyme binding requires the presence of nicotinamide part of NAD^+, while binding of ADP-ribose does not induce such change [40].

For a long time the binary complex formation between enzyme and coenzyme was described as a single-step binding mecha-

[1] These forms of enzymes will be referred to as liver alcohol dehydrogenase—LADH thorough the text.

[2] Here the term apoenzyme stands for an open conformation of LADH without NAD^+ but do not deprived of catalytic zinc.

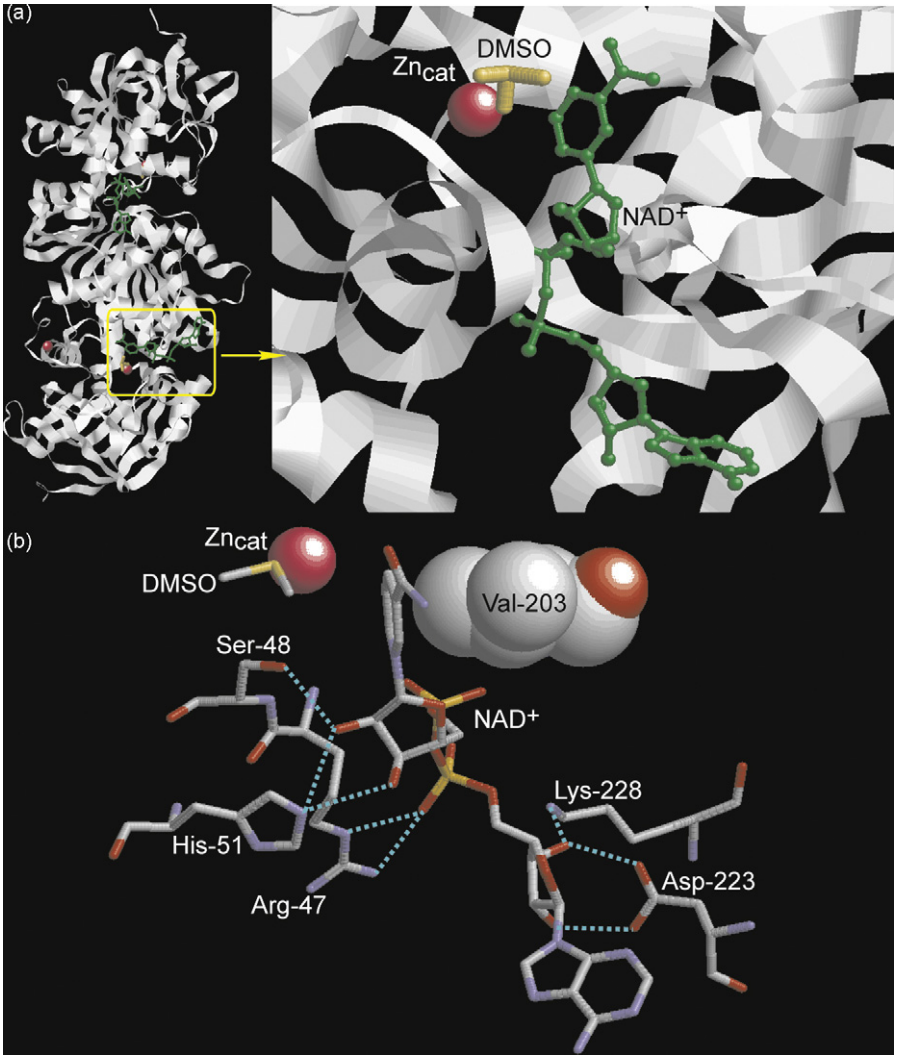

Fig. 2. Position of NAD^+ cofactor in the ternary complex with LADH: (a) overall location of NAD^+ in the enzyme, zinc is pink. DMSO, yellow. NAD^+, green; (b) NAD^+ and some of the interacting amino acid residues. For the full diagram of NAD^+–LADH interactions see [28,34]. Zinc is pink; oxygen, red; nitrogen, light blue; sulfur, yellow; phosphorus, orange; carbon, grey. Hydrogen bonds are indicated with the dashed blue lines. The figure was prepared from the PDB entry 2OHX [29] with the program RasMol.

nism [28]. At present, the conformational change during binding of NAD^+ is proposed to be a two-step process that involves binding of the AMP part of the coenzyme, followed by insertion of the nicotinamide ring close to the catalytic zinc [41]. Plapp and coworkers suggested that the change in the protein conformation forced by the NAD^+ binding coincides with the deprotonation of the enzyme–NAD^+ complex and binding of the nicotinamide ring close to the catalytic zinc–water complex. The deprotonation of the zinc-bound water, facilitated by His-51, was postulated to promote formation of the closed conformation of the enzyme–NAD^+ complex by electrostatic attraction of the positively charged nicotinamide ring of NAD^+ to the catalytic zinc-hydroxide system [41,42].

The results of transient kinetic experiments were consistent with an ordered mechanism, which requires NAD^+ to bind before alcohol. Various alcohols exert inhibitory effects on LADH. For example cyclohexanol competes for the free enzyme with NAD^+ and it forms a binary alcohol–enzyme complex with the worse affinity for NAD^+ than the enzyme alone. The same alcohol binds to enzyme-NADH to form an abortive complex, i.e. alcohol–enzyme–NADH from which the rate constant of dissociation of NADH was different from the rate determined for the binary enzyme–NADH complex [43].

2.2.2. Alcohol (substrate) binding to the catalytic zinc ion with the parallel displacement of water molecule

The LADH active site is positioned at the bottom of the domain-separating cleft about 20 Å from the LADH surface. An alcohol substrate is located in a pocket which is a continuation of the domain-separating cleft and that leads from a solution to the active-site zinc. The inner part of the pocket resembles a hydrophobic barrel formed by the amino acid residues from the catalytic domain [28]. It was shown that water is blocked off from the substrate-binding pocket by Phe-93 which is near Phe-319 [34]. Based on theoretical molecular modeling, both structural and catalytic zinc ions influence the structural integrity of the substrate-binding pocket of human alcohol dehydrogenase. The replacement of zinc atoms with different metal ions restricted the access of bulky substrates to the bottom of the active site by narrowing the bottleneck formed between Leu-116 and Val-294 [44]. The optimal binding position of the hydroxyl group occurred between 1.9 and 2.4 Å from the catalytic metal ion [45].

The substrate specificity of various MDRs depends on the dimensions and shape of the substrate channel which is adapted for small or large, and hydrophilic or hydrophobic substances by mutations or deletions/additions of amino acids [23,46]. Horse-liver alcohol dehydrogenase exhibits very broad substrate specificity

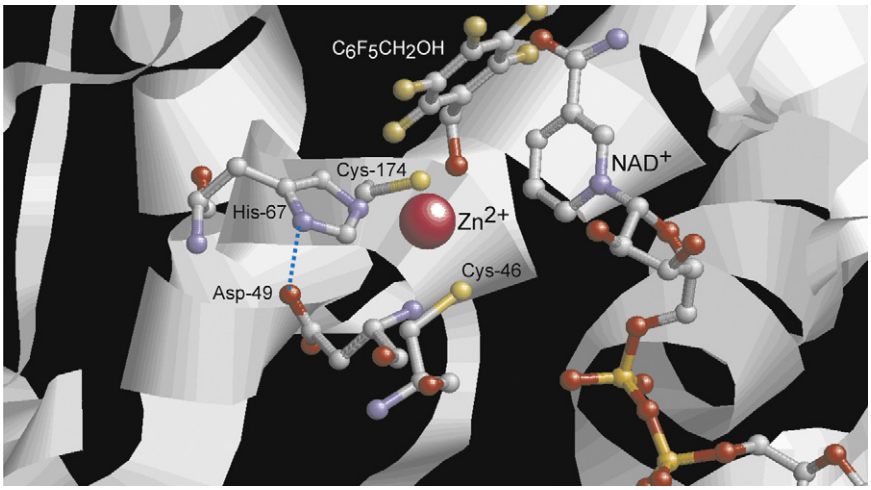

Fig. 3. The active site of LADH complexed with NAD^+ and pentafluorobenzyl alcohol. Zinc-binding residues and Asp-49 are shown. Zinc is pink, nitrogens are blue, oxygens are red and sulfurs are yellow. Hydrogen bond indicated with the blue, dashed line. The figure was prepared from the PDB entry 1HLD [34] with the program RasMol.

[47]. The amino acid residues in the substrate-binding pocket are all non-polar except Ser-48 which interacts with the hydroxyl group of the Zn-bonded alcohol. The binding of the substrate must be therefore associated with hydrophobic (van der Waals) interactions [48].

Catalytic zinc is bound to two cysteines and one histidine with the fourth coordination position being occupied by water, other ligands in solution, or a substrate molecule. The side chain of histidine is additionally positioned through a hydrogen bond between imidazole N-3 and the carboxyl group of aspartate residue (Fig. 3) [28]. Zinc is considered to act as a Lewis acid on the complexed alcohol molecule or carbonyl group of the aldehyde, facilitating the deprotonation of alcohol or nucleophilic attack on a carbonyl group. Transition metal ions of similar ionic radius and Lewis acidity such as Ni(II) or Co(II) can replace active-site zinc yielding enzymes with very similar rates of hydride transfer [49].

Variations in the zinc-binding amino acid residues in alcohol dehydrogenases of the MDR type were analyzed in detail by Auld and Bergman [50]. In general, there is a short spacer between Cys-46 and His-67 (~19 amino acids) and a long spacer segment of 106 amino acids between His-67 and Cys-174. The nature of the amino acid residues nearby the zinc ligands is highly invariant. The presence of the long spacing between the active site ligands may be important for conformational flexibility of the active-site zinc [51]. The other zinc ion, which plays the structural role in LADH, is complexed by four cysteines located within the short amino acid sequence of 15 residues (Cys-97, Cys-100, Cys-103, Cys-111) [51].

Though, it is generally accepted that an alcohol substrate in LADH is directly complexed to zinc ion during the LADH-catalyzed reaction, the removal of the molecule of water from the zinc ion during the reaction cycle has been questioned. The presence of a metal-bound water molecule in a penta-coordinate reaction intermediate was suggested on the basis of the structural studies on the Cd(II)-substituted LADH [52–54] and the EPR studies of Co(II)-substituted LADH [55]. However, it is well-known that the bigger cadmium atom usually forms complexes with a higher number of ligands than zinc (Fig. 4). Co(II) ion is also prone to expand its coordination sphere when compared to zinc. In the alcohol dehydrogenase isolated from *Thermoanaerobacter brockii*, the first metal–ligand coordination shell of Co-TbADH is distorted compared to its native (zinc) tetrahedral coordination shell and is octahedral in structure [56]. Thus the possibility could be considered that a penta-coordinate metal site would be a unique feature of Cd–LADH and Co–LADH enzymes.

The mechanism that assumes the formation of the penta-coordinate zinc intermediate was also derived from the studies on the deprotonation of the LADH–NAD^+ complex [41,42]. Similarly to the observations published by others [53], the authors of these studies proposed that the neutral alcohol could bind in the vicinity of the zinc-bound hydroxide on the same face of the zinc and donate a proton to the hydroxide ion which would then dissociate as the water molecule [41,42].

Ryde [57] considered the possibility of the inversion of zinc coordination during the catalytic reaction. There is a highly conserved glutamate residue in the second coordination sphere of zinc which is necessary for the activity of the enzyme. It is tightly kept in its position by the hydrogen bond to the glycine residue. Ryde proposed that the motion of the charged carboxylate group at Glu-68 inside the void it occupies might tune the actual partial charge on the zinc ion and speed up ligand exchange during the catalytic cycle [57]. By means of quantum chemical and molecular mechanical geometry optimizations he showed that such coordination could be accomplished with small changes in the geometry of the zinc coordination sphere and that it was kinetically favorable. The additional evidence of the dynamic role played by the conserved glutamate residue in ADHs came from the studies on ADH from *Sulfolobus solfataricus* (SsADH) [36]. Compared to its apo form, the SsADH ternary complex showed a change in the ligation state of the active-site zinc ion which was no longer bound to Glu-69. Two different coordination environments of the active-site zinc were also observed in human glutathione-dependent formaldehyde dehydrogenase FDH (also known as ADH3). In case of the FDH apoenzyme, the active-site zinc is coordinated to Cys-44, His-66 and Cys-173, and a water

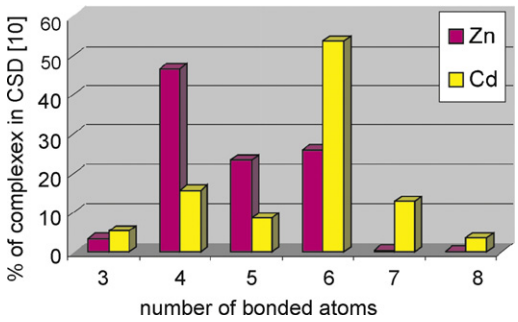

Fig. 4. The presented diagram, based on a straightforward CSD search, illustrates the tendency of cadmium ion to form six-coordinate compounds contrary to zinc, for which tetrahedral and penta-coordinate complexes prevail [10].

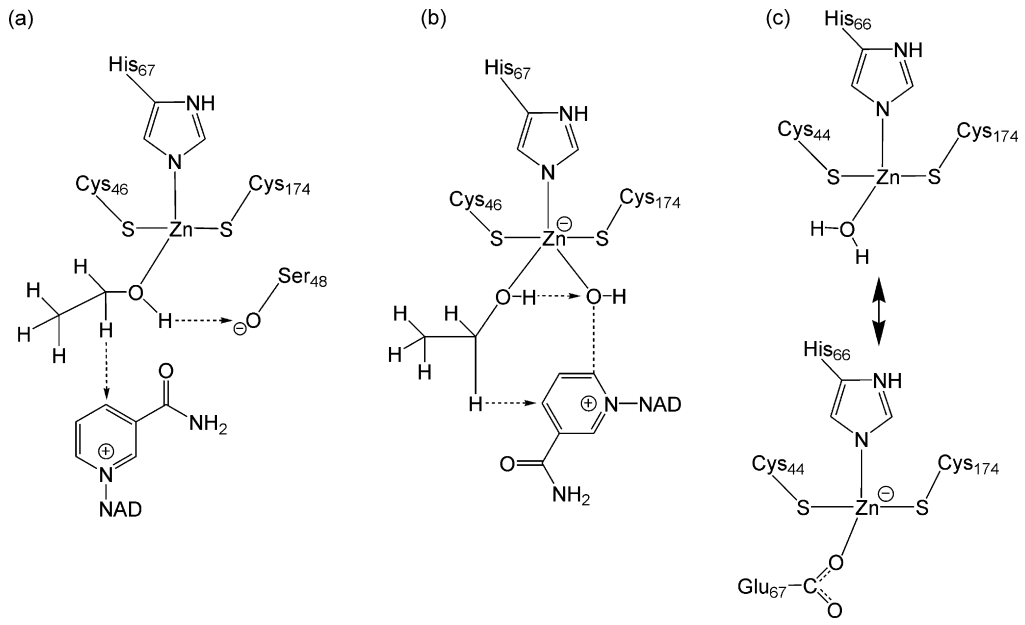

Fig. 5. Different zinc complexes postulated during the LADH-catalyzed dehydrogenation of alcohol: (a) "Classical" mechanism (e.g. [63]); (b) molecule of water takes part in the reaction [53]; (c) Glu-67 or Glu-68 can be intermittently bonded to the zinc [57,58].

molecule which is similar to the architecture found in HLADH. In the inhibited FDH·NAD(H) complex, Glu-67 is coordinated to zinc instead of a water molecule, thus zinc ions are capable of exchanging protein ligands [58].

In their very recent work Baker and co-workers [59] described the high-resolution structures of a series of binary and ternary complexes of glucose dehydrogenase (an MDR enzyme from *Haloferax mediterranei*) and showed that there were major changes in zinc coordination environment due to linked movements of the zinc ion, a zinc-bound bound water molecule, and the substrate during the reaction. These results provided a structural explanation for pentacoordinate zinc ion intermediates and highlighted the importance of dynamic fluctuations which change the electrostatic potential at the metal center and influence both the proton traffic and hydride transfer events [59].

A schematic representation of the LADH active site, as in Fig. 5 shows different complexes postulated to form during the LADH-catalyzed dehydrogenation of alcohol.

2.2.3. Dissociation and transportation of proton from alcohol hydroxyl group via the hydrogen bond network out of the catalytic site

The dissociation of a proton from the hydroxyl group of the substrate precedes and facilitates the subsequent hydride transfer. Schmidt and co-workers [60] found out that there was no solvent deuterium isotope effect on the hydride transfer step during aldehyde reduction in LADH which implies the independence of proton and hydride transfer processes. A year later, Kvassman and Pettersson [61,62] published the results of their studies on the pH dependence of the LADH reaction, and postulated a mechanism in which the deprotonation of the alcohol occurred prior to the hydride transfer. They suggested that the pK_a of the alcohol substrate was considerably lowered due to coordination to zinc, hydrogen bonding to Ser-48, and electrostatic interaction with NAD^+. According to their hypothesis, the deprotonation of the alcohol substrate facilitated the hydride transfer reaction by lowering high potential barrier for hydride dissociation. The classical molecular dynamics simulations, performed on the entire solvated LADH dimer [63], indicated that the average distance between the donor and acceptor carbon atoms for the hydride transfer step was significantly smaller after the proton relay than before the proton relay event. The activation energy barrier for hydride transfer decreased as the donor–acceptor distance decreased. Additionally the interaction of the alkoxide oxygen lone pair orbitals with zinc competed with the formation of the double bond required for the aldehyde product which resulted in an earlier, more alcohol-like transition state and a lower activation energy barrier [63].

The first three steps of the proton relay pathway, as shown in Fig. 6 include the hydroxyl groups of Ser-48, nicotinamide ribose and the imidazole ring of His-51 [63]. The protonated imidazole group can donate a proton to the bulk water [34].

2.2.4. Hydride transfer from the zinc-bound alcoholate to the nicotinamide ring of NAD^+

Hydride transfer in LADH occurs with the hydrogen tunneling effect [37,38,64] which becomes possible at a distance of approximately 2.7 Å between donor C-1 of zinc-bound alcoholate and acceptor C-4 of the nicotinamide ring of NAD^+ [38]. There is a bulky hydrophobic valine residue behind the nicotinamide ring that

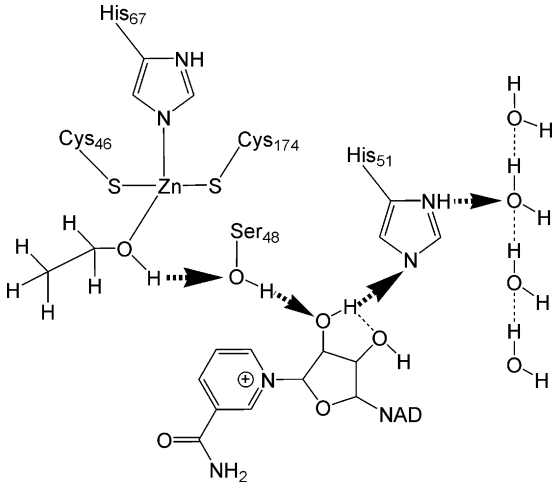

Fig. 6. Proton transfer pathway in LADH (according to [63]).

ensures a close contact between the reactive C-4 of the cofactor and C-1 of the alcohol (Fig. 2). Amino acid substitutions at Val-203 decrease the hydrogen tunneling in the reaction. In V203A mutant of HLADH the nicotinamide ring of bound cofactor moved away from C-1 of a substrate analogue, trifluoroethanol, by ~0.8 Å; this rearrangement was accompanied by a substantial decrease in the enzyme activity [37,64]. In the independent studies on T178S, V203A, V292A and V292S mutants, Plapp and co-worker showed that there were more residues in the nicotinamide binding site responsible for preorganization of the nicotinamide ring for catalysis [38].

In 2001 a group of scientist suggested that the link established between the LADH and NAD(H) activates the latter for the hydride transfer [53]. Nearly atomic resolution X-ray structures of horse-liver alcohol dehydrogenase in the complex with NAD(H) revealed the formation of an adduct in the active site between metal-bound water and NAD(H) as well as a pronounced distortion of the pyridine ring of NAD(H) [53]. The crystal structure of the Cd–DMSO–NAD(H)–LADH described by the same group in 2007, provided a picture of the ternary LADH complex just prior to the binding of DMSO (i.e. the analogue of the substrate) to the active-site metal [54]. The DMSO molecule was close enough to the active site to displace the hydroxide ion from metal ion. This displacement caused a strong interaction between NAD(H) and the hydroxide ion which distorted the nicotinamide [54]. The authors suggested that these structures demonstrated the transition state of NADH with the decreased activation energy for the transfer of a hydride [23,53,54].

Experimental evidence for the occurrence of hydrogen tunneling in natural systems has been quickly accumulating. Until 2004, this phenomenon was observed in over twenty different enzymes [65].

2.2.5. Aldehyde departure and replacement by a neutral water molecule

Product release and NADH dissociation connected with the opening of the coenzyme-binding cleft are the last steps in the catalytic cycle of alcohol dehydrogenase. However at certain aldehyde and NADH concentrations dismutation of aldehyde to alcohol and acid has been observed. Aldehyde conversion by HLADH is a rapid process [66]. Because of the slow process of NADH dissociation from the enzyme there is enough time for an aldehyde molecule to bind, and alcohol is formed. The resulting NAD^+ complex binds a new aldehyde molecule, and an acid molecule is produced [23].

2.2.6. The opening of catalytic site with the release of NADH

The breakdown of the enzyme–coenzyme complex is the rate-limiting step for LADH [67]. This is a reverse process to the NAD^+ binding, and it is connected with the isomerization of the whole enzyme from a closed to open conformation. Stopped flow kinetic studies performed for human class I liver alcohol dehydrogenase indicate that similarly to the ethanol oxidation, NADH-induced isomerization to a closed conformation may be rate-limiting for acetaldehyde reduction [68].

3. Small molecules

The zinc ion combines several features that make it suitable for both enzymatic catalysis and stabilization of protein structure. Having filled d^{10} orbitals it entirely lacks redox activity which makes it a stable ion and Lewis catalyst in a cellular environment with fluctuating redox potential. Filled d shell of zinc is also responsible for the absence of ligand field stabilization (similar to d^5 high-spin manganese(II) or d^0 magnesium(II)). The abundance of equally accessible coordination geometries makes the zinc ion an "elastic" reacting center. With its borderline hard/soft acid properties it does not show the preference for either oxygen, nitrogen or sulfur atoms. That is contrary to cadmium or mercury which bind irreversibly to the thiolate ligands. Zinc complexes exhibit a high kinetic lability which is an additional advantage in catalysis [50,69].

The small molecule models should copy the structural and spectroscopic characteristics of the first coordination sphere of zinc in natural systems. It is usually assumed that the spectroscopic features of metal ions within the protein are determined by the ligands of the first coordination sphere [70]. Thus the complexes modeling the active site of alcohol dehydrogenase are usually zinc thiolates with nitrogen donor co-ligands. Despite that, thiolates of manganese, cadmium and in particular cobalt(II) were synthesized and their NMR, EPR and electronic absorption spectra characterized to serve as a set of spectroscopic standards for Mn-, Co- and Cd-substituted LADH.

3.1. Structural and spectroscopic models of LADH active site

There are two main problems that have to be overcome during the synthesis of zinc thiolates: small zinc complexes often exhibit a coordination number exceeding four (see Fig. 4), and thiolate ligands tend to create bridges between metal ions with the formation of oligomeric species [71–73]. Two main approaches can be distinguished which lead to the construction of pseudotetrahedral environments of zinc ion in mononuclear complexes:

- the application of thiolate ligands with bulky or electron-withdrawing substituents in the vicinity of sulfur atom [11];
- the use of chelating, especially tripodal ligands which reinforce formation of mononuclear, tetrahedral zinc complexes [11,14,16,18].

There is also a combined approach, i.e. chelating ligands with sterically hindered substituents located close to the donor sulfur atom.

Several attempts to reproduce the zinc-binding centers in LADH with the model complexes that do not fit into the above scheme will be described at the end of this chapter as miscellaneous.

3.1.1. Steric thiolates and thiolates with electron-withdrawing substituents

Sterically crowded thiolates show reduced tendency to bridge metal centers [72–82]. The examples of thiols with bulky substituents, which were applied in the synthesis of mononuclear thiolate complexes, are shown in Fig. 7. Except for tri-*tert*-

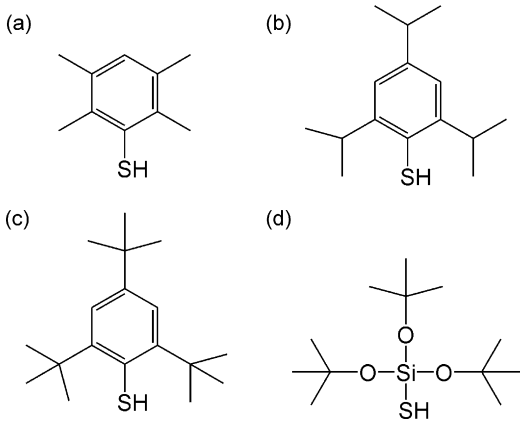

Fig. 7. The examples of sterically hindered thiols successfully applied in the syntheses of low-nuclearity zinc complexes: (a) 2,3,5,6-Me_4C_6HSH [74]; (b) 2,4,6-$i Pr_3C_6H_2SH$ [74]; (c) 2,4,6-$t Bu_3C_6H_2SH$ (e.g. [79]); (d) $(t BuO)_3SiSH$ (e.g. [94]). For review see [73].

butoxysilanethiol, these compounds are all arenethiols. The use of ligands with the extreme steric hindrance close to the donor sulfur atom allowed the formation of three- and even two-coordinate zinc thiolates [78,80–82].

The first stable aldehyde and ketone complexes of zinc were formed during the synthesis of zinc 2,4,6-tri-*tert*-butylthiophenolate and its selenium analogue. Despite the presence of voluminous *tert*-butyl substituents close to the donor atom of thiolate/selenolate ligand, the crystal structure of zinc selenolate with p-anisaldehyde as a co-ligand revealed a dimeric nature of the complex (Fig. 8a, Table 2) [79]. The same authors described the reactions of $(2,4,6\text{-}t\mathrm{Bu}_3\mathrm{C}_6\mathrm{H}_2\mathrm{S})_2\mathrm{Zn}$ and $(2,4,6\text{-}t\mathrm{Bu}_3\mathrm{C}_6\mathrm{H}_2\mathrm{Se})_2\mathrm{Zn}$ with pyridine and imidazole-based nitrogen ligands. Several, three- and four-coordinate zinc complexes were synthesized including a complex with an S_2NO ligand environment which crystallized after the addition of pyridine carboxaldehyde to the solution of $(2,4,6\text{-}t\mathrm{Bu}_3\mathrm{C}_6\mathrm{H}_2\mathrm{S})_2\mathrm{Zn}$. On the basis of IR spectrum the chelating nature of the pyridinecarboxaldehyde ligand in the complex was established however the crystal structure of $\mathrm{Zn}(2,4,6\text{-}t\mathrm{Bu}_3\mathrm{C}_6\mathrm{H}_2\mathrm{S})_2(\mathrm{NC}_5\mathrm{H}_4\mathrm{CHO})$ was not determined [80].

Monomeric four- and five-coordinate cobalt complexes with thiolate and nitrogen ligands were obtained by the reaction of $\mathrm{Co}(\mathrm{S}\text{-}2,4,6\text{-}i\text{-}\mathrm{Pr}_3\mathrm{C}_6\mathrm{H}_2)_2$ or $\mathrm{Co}(\mathrm{S}\text{-}2,6\text{-}i\text{-}\mathrm{Pr}_2\mathrm{C}_6\mathrm{H}_3)_2$ with pyridine, bipyridine, phenantroline or 1-methylimidazole in acetonitrile. When the same reaction was performed with a less sterically hindered thiolate ligand, i.e. 2,3,5,6-tetramethyl-benzenethiolate, the resultant complex was a dimer [74]. The electronic absorption spectra of $[\mathrm{Co}(\mathrm{S}\text{-}2,4,6\text{-}iso\text{-}\mathrm{Pr}_3\mathrm{C}_6\mathrm{H}_2)_2(1\text{-Meimid})]$ in toluene and acetonitrile showed energies and intensities of the ligand field bands consistent with tetrahedral coordination, whereas the electronic spectra of $[\mathrm{Co}(\mathrm{S}\text{-}2,4,6\text{-}iso\text{-}\mathrm{Pr}_3\mathrm{C}_6\mathrm{H}_2)_2(\mathrm{bpy})(\mathrm{CH}_3\mathrm{CN})]$ and its phen analogue in acetonitrile showed markedly reduced intensity for the ligand field bands in the visible and near-infrared regions consistent with five-coordination of metal ion. It was suggested that these complexes could serve as a spectroscopic reference for the coordination state of cobalt-substituted catalytic center in LADH [74].

The bridging tendency of thiolates can be markedly reduced by applying electronegative substituents, as in pentafluorothiophenolate [83]. The coordination $\mathrm{ZnNS_2O}$, which represents the enzyme–substrate complex of alcohol dehydrogenase, was for the first time realized when zinc pentafluorothiophenolate was reacted with chelating alcohols and aldehydes [75]. Both zinc–alcohol and zinc–aldehyde ligation were structurally characterized in heteroleptic complexes featuring coordination environments: $\mathrm{ZnNS_2O}$, $\mathrm{ZnN_2S_2}$, and $\mathrm{ZnNS_2O_2}$. The complexes of $\mathrm{Zn}(\mathrm{SC_6F_5})_2$ with picoline-2-methanol and picoline-2-carbaldehyde exhibited high structural similarity pointing to sterically unrestricted exchange between corresponding alcohols and aldehydes in the ligand sphere of zinc (Fig. 8b and c, Table 2) [75].

In their review on the complexes of sterically hindered thiolate ligands Dilworth and Hu suggested that the advent of silyl thiols possessing Si–SH functional group might be an incentive for the further studies in the area of monomeric thiolate metal

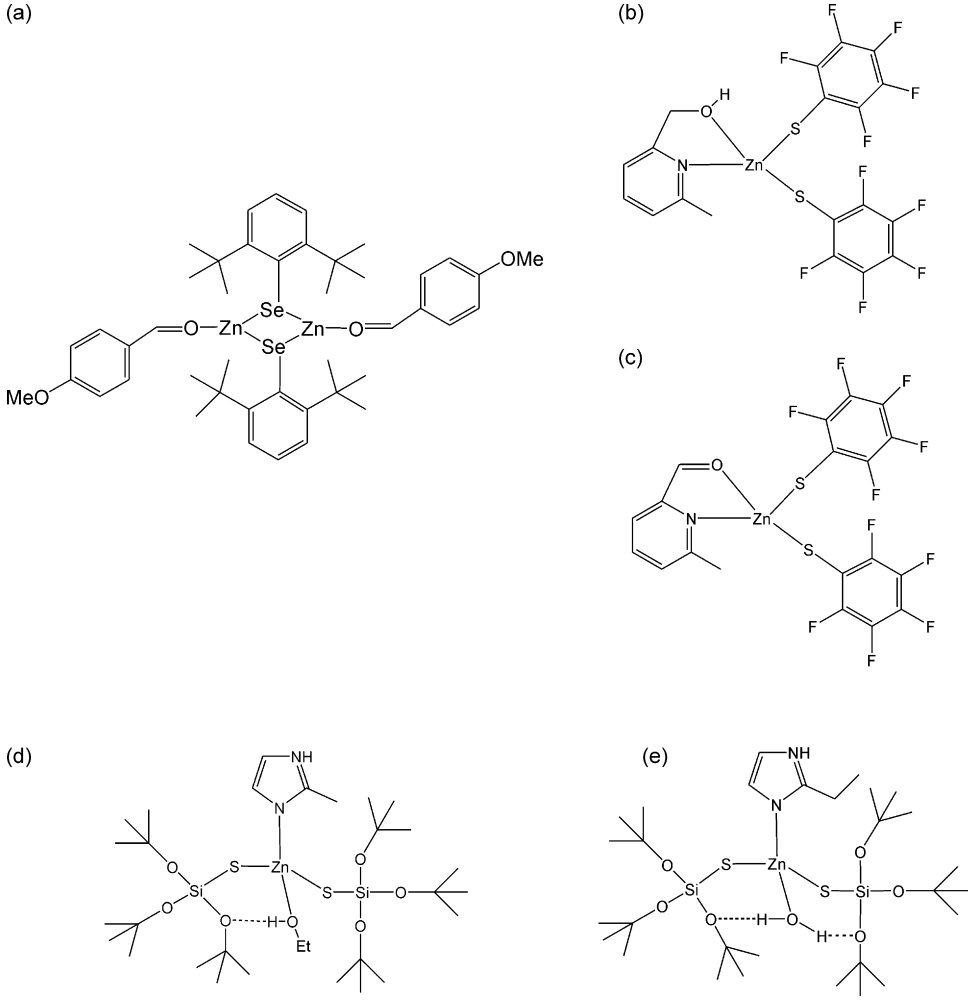

Fig. 8. Examples of zinc complexes featuring bulky thiolate ligands: (a) $[(p\text{-}\mathrm{MeOC_6H_4CHO})\mathrm{Zn}(2,4,6\text{-}t\mathrm{Bu}_3\mathrm{C}_6\mathrm{H}_2\mathrm{Se})_2]_2$ [79]; (b) $[(\mathrm{PicMeOH})\mathrm{Zn}(\mathrm{SC_6F_5})_2]$ [75]; (c) $[(\mathrm{PicCHO})\mathrm{Zn}(\mathrm{SC_6F_5})_2]$ [75]; (d) $\{(2\text{-MeIm})(\mathrm{C_2H_5OH})\mathrm{Zn}[\mathrm{SSi}(\mathrm{O}t\mathrm{Bu})_3]2\}$ [94]; (e) $\{(2\text{-EtIm})(\mathrm{H_2O})\mathrm{Zn}[\mathrm{SSi}(\mathrm{O}t\mathrm{Bu})_3]_2\}$ [92].

Table 2
Important bond lengths in model complexes and LADH active site.

Formula/PDB symbol	Zn–S [Å]	Zn–N [Å]	Zn–O [Å]	[Ref.]	Zinc coord.	Comments
Protein						
1HLD	2.19	2.21	2.05	[34]	$ZnNOS_2$	Ternary complex with NAD^+ and PFB, homodimer
	2.23	2.23	2.04			
	2.20			[29]	$ZnNOS_2$	Ternary complex with NAD^+ and DMSO, homodimer
	2.30					
2OHX	2.19	2.14	2.26			
	2.23	2.02	2.13			
	2.25					
	2.32					
1YE3	2.21	2.05	2.11	[178]	$ZnNOS_2$	Ternary complex with NAD^+ and water, monomer
	2.42					
Model complexes						
Water						
{(2-EtIm)(H_2O)[SSi(O*t*Bu)$_3$]$_2$Zn}	2.3070(5)	2.0310(15)	2.0449(13)	[92]	$ZnNOS_2$	Monomeric, also Co(II) analog.
	2.2758(5)					
$Tp^{Pic,Me}Zn(H_2O)[PO_2(OC_6H_5)_2]$	–	2.065(4)	1.947(3) P	[120]	ZnN_3O_2	Monomeric, neutral
		2.069(4)	2.102(3) w			
		2.200(4)				
$[(Tp^{CO2Et,Me})Zn(OAc)(H_2O)]$		2.040(5)	2.014(4) ac	[122]	ZnN_3O_2	Monomeric, neutral
		2.076(4)	1.966(4) w			
		2.376(5)				
$[(Tp^{tBuA,Me})(H_2O)Zn]](ClO_4)$		2.024(3)	2.190(3) c	[123]	ZnN_2O_3	Monomeric, cationic
		2.019(3)	2.276(3) c			
			1.922(3) w			
$(X_6Et_3Imet_3)(H_2O)Zn](ClO_4)_2\cdot(H_2O)$	–	1.997(4)	1.972(4)	[134]	ZnN_3O	Monomeric, dicationic
		1.985(2)				
		2.011(3)				
$[(TriMim)(H_2O)Zn](BF_4)_2$	–	2.01(1)	2.13(1)	[145]	ZnN_3O	Monomeric, dicationic
		2.00(1)				
		2.00(1)				
Hydroxide						
$\{[(bmnpa)(OH)Zn](ClO_4)\}_2$	2.514(1)	2.189(3)	2.028(3)	[126]	ZnN_2O_2S	Dimer, cationic
		2.068(2)	1.974(3)			
$[(ebnpa)(OH)Zn](ClO_4)$	2.533(1)	2.077(2)	1.925(2)	[127]	ZnN_3OS	Monomeric, cationic
		2.193(2)				
		2.109(2)				
Alcohols						
$(PicMeOH)Zn(SC_6F_5)_2$	2.249(1) 2.290(1)	2.048(3)	2.123(3)	[75]	$ZnNOS_2$	Monomeric, chelate N,O
{(2-MeIm)(EtOH) [SSi(O*t*Bu)$_3$]$_2$Zn}	2.2826(11)	2.002(13)	2.143(3)	[94]	$ZnNOS_2$	Monomeric, co-crystal
	2.2818(12)					
{(2-MeIm)(MeOH)[SSi(O*t*Bu)$_3$]$_2$Zn}	2.2851(7)	2.004(2)	2.1359(19)	[94]	$ZnNOS_2$	Monomeric, also Cd(II) analog.
	2.2792(8)					
$[HB(mim^{o\text{-}An})_2(pz^{Ph,Me})(EtOH)Zn](ClO_4)\cdot EtOH$	2.282(1)	2.012(3)	1.970(3)	[107]	$ZnNOS_2$	Monomeric, cationic
	2.314(1)					
$[(Tm^{Mes})(MeOH)Zn](ClO_4)\cdot MeOH$	2.313(1)	–	1.993(3)	[102]	$ZnOS_3$	Monomeric, cationic
	2.338(1)					
	2.320(1)					
$[(Tm^{p\text{-}Tol})(i\text{PrOH})Zn](ClO_4)\cdot(i\text{PrOH})$	2.307(2)	–	1.979(4)	[113]	$ZnOS_3$	Monomeric, cationic
	2.317(2)					
	2.332(2)					
$[(Tm^{p\text{-}Tol})(i\text{PrOH})Zn](ClO_4)$	2.309(2)	–	1.984(4)	[113]	$ZnOS_3$	Monomeric, cationic
	2.315(2)					
	2.332(2)					
$[(bmapa)(MeOH)Zn](ClO_4)_2\cdot MeOH$	2.434(1)	2.054(2)	2.077(1)	[124]	ZnN_2OS_2	Monomeric, cationic
	2.452(1)	2.163(2)				
Aryloxides						
$[(bmnpa)(p\text{-}NO_2C_6H_5O)Zn](ClO_4)$	2.4766(8)	2.207(2)	1.950(2)	[128]	ZnN_2OS_2	Monomeric, cationic
	2.4529(9)	2.068(2)				
$[(bmnpa)(p\text{-}CNC_6H_5O)Zn](ClO_4)$	2.4483(8)	2.198(2)	1.942(2)	[128]	ZnN_2OS_2	Monomeric, cationic
	2.4853(9)	2.096(2)				
$[(X_6Et_3Imet_3)(EtOH)Zn](ClO_4)_2$	–	1.978(5)	1.972(4)	[136]	ZnN_3O	Monomeric, dicationic
		1.977(5)				
		1.989(5)				

Table 2 (*Continued*)

Formula/PDB symbol	Zn–S [Å]	Zn–N [Å]	Zn–O [Å]	[Ref.]	Zinc coord.	Comments
Alkoxides						
[($Tp^{tBu,Me}$)(EtO)Zn]	–	2.0592(13) 2.052(14) 2.0676(14)	1.825(2) 1.826(2) Disorder	[115]	ZnN_3O	Monomeric, neutral
[Zn(OMe)L](BPh_4); L = *cis*,*cis*-1,3,5-tris[(*E*,*E*)-3-(2-furyl)acrylidene-amino]cyclohexane	–	2.016(12) 2.032(10) 2.070(9)	1.896(10)	[118]	ZnN_3O	Monomeric, cat. co-crystal with Zn-hydroxide complex
[($Tp^{Cum,Me}$)($Cl_3CCH(OH)O$)Zn]	–	2.063(3) 2.063(3) 2.040(3)	1.865(2)	[109]	ZnN_3O	Monomeric, neutral α-hydroxy-alkoxide
[($Tp^{Cum,Me}$)($C_6H_4(CHO)O$)Zn]	–	2.213(2) 2.038(2) 2.046(2)	1.904(2) ph 2.173(2) a	[109]	ZnN_3O_2	Monomeric, neutral chelate formylphenol
[($Tm^{2,6\text{-}Xy}$)Zn(MeO)Zn($Tm^{2,6\text{-}Xy}$)]	2.35(2)	–	1.957(5) 1.941(5)	[113]	$S_3Zn–O–ZnS_3$	Dimer, cationic, bridging alkoxide
[($Tm^{2,6\text{-}Xy}$)Zn(EtO)Zn($Tm^{2,6\text{-}Xy}$)]	2.36(2)	–	1.959(3) 1.967(3)	[113]	$S_3Zn–O–ZnS_3$	Dimer, cationic, bridging alkoxide
[(ebnpa)(CH_3O)Zn](ClO_4)	2.490(3)	2.212(10) 2.076(9) 2.095(8)	1.953(8)	[127]	ZnN_3OS	Monomeric, cationic
Aldehydes						
[(*p*-$MeOC_6H_4CHO$)(2,4,6-$tBu_3C_6H_2Se)_2$Zn]$_2$	2.345(3)[b] 2.552(4)[t]	–	2.059(7)	[79]	$ZnOSe_3$	Dimer, selenolate
[(PicCHO)($SC_6F_5)_2$Zn]	2.256(7) 2.250(8)	2.07(1)	2.24(1)	[75]	$ZnNOS_2$	Monomeric, chelate N,O
[($X_6Et_3Imet_3$)(CH_3CHO)Zn]($ClO_4)_2$	–	1.969(6) 1.994(6) 1.987(6)	1.882(8)	[137]	ZnN_3O	Monomeric, dicationic
Other						
[(MIEH)($H_2N(CH_2)_2OH$)Zn]	2.314(4)	2.20(1) 2.19(1)	1.95(1) 2.08(1)	[149]	ZnN_2O_2S	Monomeric, neutral

complexes [84]. Since 1974, when the first paper on the synthesis of trialkoxysilanethiolates of alkali and alkali-earth metals was published [85], almost 200 metal complexes possessing M–S–Si bond were structurally characterized [10]. Initially, zinc tri-*tert*-butoxysilanethiolates were described in 1996 by Becker et al. [86]. One of those compounds – with the zinc-coordinated acetonitrile – was the first from the family of complexes with $ZnNO_2S_2$ coordination which was later described in several papers. In 2001 the first example of the crystal structure of the aqua-ligated zinc thiolate was published. In this bimetallic complex both zinc ions exhibited tetrahedral geometry with one of them surrounded by two thiolates and two water molecules [87]. In 2002 a tetrahedral cobalt(II) complex with $CoNOS_2$ core, i.e. [Co{$SSi(OtBu)_3$}$_2$(H_2O)(2-methylpyridine)] was identified by UV–vis measurements carried out for [Co{$SSi(OtBu)_3$}$_2$(2-methylpyridine)] in THF/H_2O and isopropanol/H_2O [88].

The combination of various imidazole derivatives with tri-*tert*-butoxysilanethiolate ligand in zinc, cobalt(II), manganese and cadmium complexes led to the formation of very close structural analogues of LADH active site including the complexes with water and alcohols (Fig. 8d and e, Table 2) [89–94]. The complexation of O-ligands (water, methanol, ethanol) within the complexes was stabilized by the intramolecular hydrogen bonds (Table 3) [89,92–95]. The synthesis of Co(II) and Cd(II) analogues of zinc tri-*tert*-butoxysilanethiolates with imidazole co-ligands allowed for the comparison of UV–Vis and ^{113}Cd NMR spectra of metal ions in NOS_2 and NO_2S_2 environment of ligands with the spectra of Co(II)- and Cd(II)-substituted LADH [94,96,97]. The results of crystallographic studies, supported by solid state NMR strongly indicated that zinc in LADH–NAD(H) complex is surrounded by five ligands including two O-ligands. When Zn is replaced by cadmium, the architecture of the complex remains basically the same [94–97]. Isomorphous zinc(II) and cobalt(II) tri-*tert*-butoxysilanethiolates with 2-ethylimidazole and water as co-ligands were synthesized, and some properties of water complexed to zinc or cobalt ion in an environment mimicking LADH active site were studied. It was concluded that there should be no substantial differences between zinc and cobalt-substituted systems (Table 3). Moreover, the FT-IR spectra of the complexes confirmed slightly higher acidity of water bonded to the cobalt ion [92]. The comparison of hydrogen bonds formed by O-ligands in the heteroleptic zinc tri-*tert*-butoxysilanethiolates shows shortening of the hydrogen bond formed by alcohol compared to the H-bonds formed by the molecule of water (~0.05 Å) [92,94]. The same situation indicating the increased acidity of alcohol as compared to water was observed in the case of cobalt silanethiolates with water and methanol as co-ligands [92,95].

3.1.2. Chelating ligands and combination of chelating effect with steric hindrance

The use of chelating, especially tripodal ligands in the synthesis of low-nuclearity metal complexes was previously reviewed in 1999, 2000 and 2004 by Vahrenkamp and Parkin [11,12,14]. This approach was purposefully applied to model the active site of LADH in 1981. A series of thioethers and thiol-containing ligands was synthesized (Fig. 9) and their coordination behaviour towards Co^{2+}, Zn^{2+}, Cu^{2+}, Ni^{2+} was studied. The ligands containing pyridine and two thioether molecules did not bind divalent metals strongly, whereas their analogues containing free mercapto

Table 3
Hydrogen bonding formed by the O-ligand within the model complex with various acceptors.

Formula/PDB symbol	Acceptor X	O. . .X dist. [Å]	Ref.	Zinc coord.	Comments
$[HB(mim^{o\text{-}An})_2(pz^{Ph,Me})(EtOH)Zn](ClO_4)\cdot EtOH$	O(EtOH)	2.573(2)	[107]	$ZnNOS_2$	Monomeric, cationic
$[(Tm^{Mes})(MeOH)Zn](ClO_4)\cdot MeOH$	O(MeOH)	2.577	[102]	$ZnOS_3$	Monomeric, cationic
$[(Tm^{p\text{-}Tol})(i\text{PrOH})Zn](ClO_4)\cdot(i\text{PrOH})$	O(*i*PrOH)	2.67	[113]	$ZnOS_3$	Monomeric, cationic
$[(Tm^{p\text{-}Tol})(i\text{PrOH})Zn](ClO_4)$	$O(ClO_4^-)$	2.84	[113]	$ZnOS_3$	Monomeric, cationic
$\{(Tp^{Pic,Me})(H_2O)[PO_2(OC_6H_5)_2]Zn\}$	O (O_3PO)	2.771	[120]	ZnN_3O_2	Monomeric, neutral
	N	2.745			
$[(Tp^{CO2Et,Me})(OAc)(H_2O)Zn]$	O (CO_2Et)	2.661	[122]	ZnN_3O_2	Monomeric, neutral
	O (AcO)	2.526			
$(Tp^{tBuA,Me})(H_2O)Zn(ClO_4)$	O (CONH)	2.586(5)	[123]	ZnN_2O_3	Monomeric, cationic
	O	2.918			
$[(bmapa)(MeOH)Zn](ClO_4)_2\cdot MeOH$	O(MeOH)	2.58	[124]	ZnN_2OS_2	Monomeric, cationic
$[(bmnpa)(OH)Zn](ClO_4)_2$	$O(ClO_4^-)$	2.90	[126]	ZnN_2O_2S	Dimer, cationic
$[(ebnpa)(OH)Zn](ClO_4)$	$O(ClO_4^-)$	3.03	[127]	ZnN_3OS	Monomeric, cationic
$[(X_6Et_3Imet_3)(H_2O)Zn](ClO_4)_2\cdot(H_2O)$	O(ether)	2.82	[134]	ZnN_3O	Monomeric, dicationic
	O(water)	2.539(7)			
$[(X_6Et_3Imet_3)(EtOH)Zn](ClO_4)_2$	O(ether)	2.86	[136]	ZnN_3O	Monomeric, dicationic
$\{(2\text{-EtIm})(H_2O)[SSi(O\text{t}Bu)_3]_2Zn\}$	O	2.7244(19)	[92]	$ZnNOS_2$	Monomeric, also Co(II) analog.
		2.7039(19)			
$\{(2\text{-MeIm})(EtOH)[SSi(O\text{t}Bu)_3]_2Zn\}$	O	2.659(4)	[94]	$ZnNOS_2$	Monomeric
$\{(2\text{-MeIm})(MeOH)[SSi(O\text{t}Bu)_3]_2Zn\}$	O	2.676(3)	[94]	$ZnNOS_2$	Monomeric, also Cd(II) analog.

groups bound these metals very strongly and produced complexes which were probably neutral bis-thiolates. The formation of the neutral complexes with ZnS_2N coordination was suggested [98].

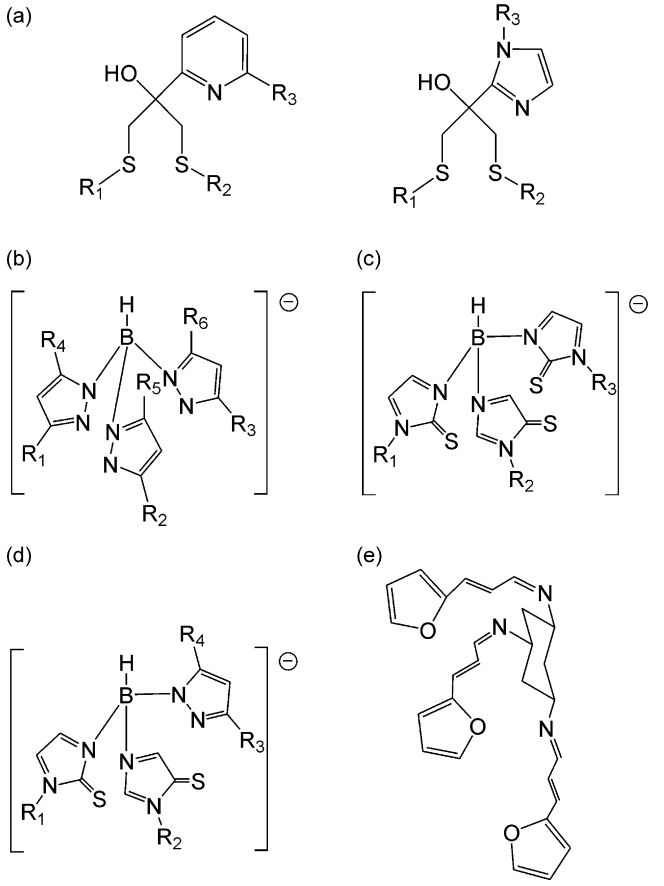

Fig. 9. The chelating N/S-ligands (I): (a) first chelates designed to synthesize synthetic models of LADH [98]; (b) tris(pyrazolyl)hydroborates: $R_1 = R_2 = R_3 =$ Cum, $R_4 = R_5 = R_6 =$ Me [114], $R_1 = R_2 = R_3 = t$Bu, $R_4 = R_5 = R_6 =$ Me [115], $R_1 = R_2 = R_3 =$ Pic, $R_4 = R_5 = R_6 =$ Me [120], $R_1 = R_2 = R_3 = CO_2Et$, $R_4 = R_5 = R_6 =$ Me [122], $R_1 = R_2 = R_3 =$ Py, $R_4 = R_5 = R_6 =$ Me [123], $R_1 = R_2 = R_3 = t$BuA, $R_4 = R_5 = R_6 =$ Me [123]; (c) tris(mercapto)hydroborates: $R_1 = R_2 = R_3 =$ Mes [102], $R_1 = R_2 = R_3 = t$Bu, Cum [103]; (d) bis(mercapto)pyrazolyl-hydroborates: $R_1 = R_2 =$ Me, $R_3 = R_4 =$ H [110], $R_1 = R_2 = o$-An, $R_3 =$ Ph, $R_4 =$ Me [107]; (e) *cis*, *cis*-1,3,5-tris[(*E*,*E*)-3-(2-furyl) acrylidene-amino]cyclohexane [118].

3.1.2.1. Tris(pyrazolyl)borates Tp^R, tris(mercaptoimidazolyl)hydroborates Tm^R and cis,cis-1,3,5-tris[(E,E)-3-(2-furyl)acrylidene-amino] cyclohexane. The compounds most widely used in the synthetic bioinorganic chemistry are undoubtedly derivatives of N-donor tris(pyrazolyl)hydroborate with substituents R attached at the position 3 of the pyrazole rings [11,12,99,100] and soft S-donor tris(mercaptoimidazolyl)hydroborates with the substituents at the N-1 atom of thioimidazole [11,12,18,101–103]. The special issue of Inorganica Chimica Acta in 2009 was dedicated to Swiatoslaw Trofimenko who was the first to synthesize and explore the coordination chemistry of pyrazolylborates [104]. The choice of tris(pyrazolyl)hydroborate, tris(mercaptoimidazolyl) (or tris(thioimidazolyl)hydroborate) ligands as well as the mixed derivatives with N,S-donor atoms are presented in Fig. 9. A complete series of tripod zinc complexes, in which the pyrazolyl/mercaptoimidazolylborate-derived tripods possessed N_3, N_2S, NS_2, and S_3 donor sets, was investigated. In those ligands the pyrazole ring and thioimidazole mimic histidine and cysteine, respectively, both amino acids being present in the enzymes and acting as donor systems that bind zinc. The great advantage of the tripods is that they are permanently attached to zinc in solutions, enabling studies on the interconversions of their complexes [102,103,105–109]. Encapsulating tris(pyrazolyl)hydroborate (Tp^R) and tris(2-mercaptoimidazolyl)hydroborate (Tm^R) ligands as well as mixed pyrazolylmercaptoimidazolylborates allowed for the synthesis of structural models and mechanistic investigations of enzyme-like situations. Water and all LADH substrates, i.e. alcohols, alkoxides and aldehydes had been attached to zinc ions together with the tripods [102,103,107–109].

The first mixed N,S,S ligand designed to reproduce the sulfur-rich composition of the LADH active site was reported in 1997 by Parkin and co-workers [110]. The molecular structure of [bis(2-mercapto-1-methylimidazolyl)(pyrazolyl)hydroborato]zinc complex was determined and the coordination geometry about zinc compared with the coordination of zinc in the active site of LADH [110]. The increase of the steric hindrance of the N,S,S ligand, by the application of 1-(o-anisyl) substituent led to the formation of the first zinc complex in which the N,S,S ligation of zinc and the attachment of ethanol occurred [107,108]. The structural details of the $ZnNS_2O$ coordination in the complex and in DMSO-inhibited ADH were reported to be in a good agreement. The alcohol ligand was embedded between the three aromatic substituents of the chelating anion and attached to a second ethanol molecule by a hydrogen bond (Fig. 10a, Tables 2 and 3) [107,108].

Interestingly, the use of a less sterically crowded tris(2-mercapto-1-methylimidazolyl)hydroborate ligand resulted in the formation of an entirely different ZnS_4 complex [111].

Alcohol ligation was also described for zinc complexes with *N*-*tert*-butyl- and *N*-4-cumenyltris(2-mercaptoimidazyl)hydroborate ligands [103] as well as tris(2-mercapto-1-mesityl-imidazolyl)borate ligand [102]. The coordination geometry of zinc in the cationic tris(2-mercaptoimidazolyl)hydroborate complexes with methanol [102] and ethanol [103] resembles aspects of that in LADH. The Zn–O and Zn–S bond lengths (collected in Table 2) are comparable to those in the NAD^+–alcohol–LADH ternary complexes. The hydroxyl group of the coordinated alcohol both in $\{[Tm^{Mes}]Zn(MeOH)\}^+$ (Fig. 10b) [102] and $\{[Tm^{tBu}]Zn(EtOH)\}^+$ [103] participates in the hydrogen-bonding interaction with an additional molecule of alcohol. The authors suggested that this interaction mimicked the hydrogen bond that is present in the LADH active site. The donor-to-acceptor O···O separation between alcohol molecules (2.58 Å for methanol [102] and 2.657(3) Å for ethanol complex [103]) was similar to that between the zinc-bound alcohol in the LADH active site and Ser-48 (Table 3 [34,112]). Finally, zinc complexes of 2-propanol were obtained with the use of new tris[2-mercapto-1-(2′,6′-xylylimidazolyl)]hydroborate ligand [113]. Contrary to methanol, 2-propanol was preferred over perchlorate as a donor, however equilibrium mixtures of alcohol and perchlorate complexes were suggested to exist in solution (Tables 2 and 3) [113].

The stable aryloxide as well as alkoxide zinc species, which are proposed to be the reactive moieties for hydride transfer to NAD^+ during alcohol oxidation in the liver alcohol dehydrogenase (LADH), were first obtained in the reaction of the $Tp^{Cum,Me}$Zn-OH complex with the respective phenols or alcohols in dichloromethane [114]. The reaction was initially observed only for alcohols bearing electronegative substituents including trichloroethanol and trifluoroethanol [114]. However, the presence of simple methoxide, ethoxide and isopropoxide derivatives at the exchange with $Tp^{tBu,Me}$Zn-OH was soon evidenced by NMR stud-

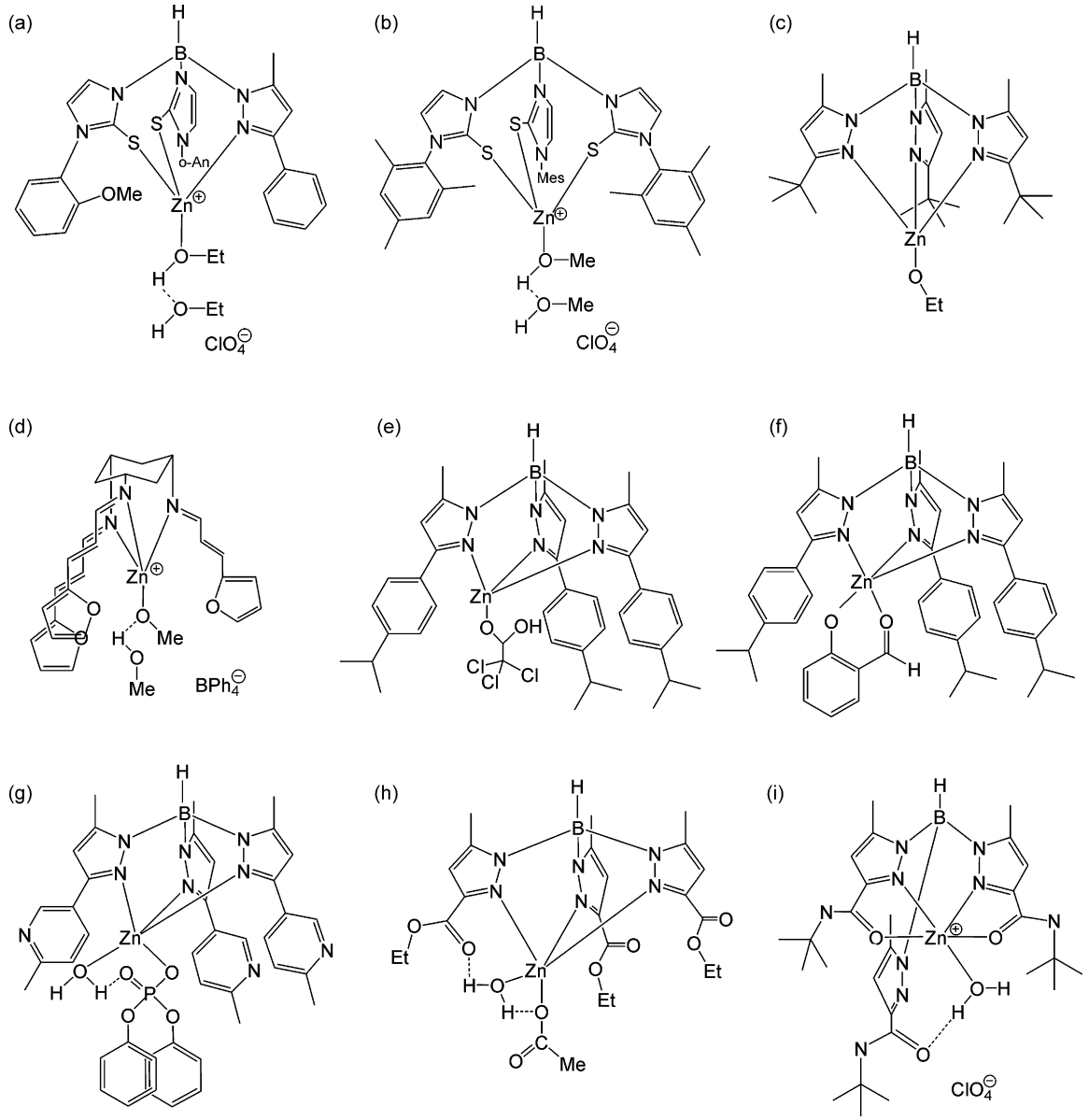

Fig. 10. Zinc complexes with the chelating N/S-ligands (I): (a) $[HB(mim^{o\text{-}An})_2(pz^{ph,Me})(EtOH)Zn]ClO_4{\cdot}EtOH$ [107]; (b) $[(Tm^{Mes})(MeOH)Zn]ClO_4{\cdot}MeOH$ [102]; (c) $[(Tp^{tBu,Me})(EtO)Zn]{\cdot}0.5C_7H_8$ [115]; (d) part of $[Zn(OMe)L]{\cdot}[Zn(OH)L](BPh_4)_2{\cdot}1.8MeOH{\cdot}0.8CH_2Cl_2$; L = *cis*,*cis*-1,3,5-tris[(*E*,*E*)-3-(2-furyl)acrylidene-amino]cyclohexane [118]; (e) $[(Tp^{Cum,Me})(Cl_3CCH(OH)O)Zn]{\cdot}2CH_3CN{\cdot}2H_2O$ [109]; (f) $[(Tp^{Cum,Me})(C_6H_4(CHO)O)Zn]$ [109]; (g) $\{(Tp^{Plc,Me})(H_2O)[PO_2(OC_6H_5)2]Zn\}$ [120]; (h) $[(Tp^{CO2Et,Me})(OAc)(H_2O)Zn]$ [122]; (i) $[(Tp^{tBuA,Me})(H_2O)Zn]ClO_4{\cdot}0.5CH_2Cl_2$ [123].

ies [115]. Both the methoxide [116] and ethoxide [116] complexes were isolated by a different synthetic method, i.e. the alcoholysis of $Tp^{R}Zn$-hydride (Fig. 10c). Zn–O bonds in all the obtained complexes were extremely short (Table 2) [115,116].

Factors influencing the formation of tetrahedral alkoxide complexes were studied by applying a combination of experimental and theoretical approach to the reactions of the tris(pyrazolyl)hydroborato zinc-hydroxide complexes with alcohols [117]. Zinc alkoxide formation was favored by electron-withdrawing substituents in the alcohol and sterically disfavored for bulky alkoxides. Almost all the zinc alkoxide complexes with the exception of derivatives of acidic alcohols turned out to be hydrolytically unstable. The active site environment of LADH was suggested to play an important role in stabilizing the alkoxide intermediate, possibly *via* hydrogen-bonding interactions [117]. This hypothesis was nicely supported by the model studies of Cronin and Walton [118]. They described the direct reaction of the hydroxide complex with methanol to give the methoxide complex. The model reaction was achieved within a zinc complex of *cis*,*cis*-1,3,5-tris[(*E*,*E*)-3-(2-furyl)acrylidene-amino]cyclohexane (Fig. 9). $[Zn(OMe)L]^+$ co-crystallized with $[Zn(OH)L]^+$ with the three pendant 'arms' of the ligand creating an encapsulating environment around the hydroxide or methoxide ion (Fig. 10d). Methanol solvent molecule, which was present within the deep cavity, interacted with the methoxide *via* a hydrogen bond with donor acceptor distance O···O 2.679(11) Å similar to hydrogen bonds detected in tris(pyrazolyl)borate and tris(2-thioimidazolyl)hydroborate complexes and in the active site of liver alcohol dehydrogenase (Table 3). The short Zn–O distance was consistent with the distances reported for other zinc-alkoxide species (Table 2). The exchange of hydroxide for methoxide within the complex indicated increased stability of the alkoxide complex in the hydrophobic environment formed by the ligand [118]. Cationic cobalt phenoxide and ethoxide complexes of the same ligand were obtained and structurally characterized. The electronic absorption spectra of the phenoxide complex in an inert gas atmosphere were reported [119].

The first phenoxide derivative of a tris(2-mercaptoimidazolyl)hydroborate zinc species, imitating sulfur-rich coordination of zinc in LADH, was reported in 2001 [103]. The incorporation of *p*-nitrophenolate was described for zinc complexed to *N*-4-cumenyltris(2-mercaptoimidazyl)hydroborate. This molecular species turned out to be thermally and hydrolytically stable. The Zn–O bond was certainly shorter than the Zn–O bonds formed by neutral alcohol molecules (Table 2) [103]. Singly bridging methoxide and ethoxide derivatives of a tris(2-mercaptoimidazolyl)hydroborate zinc complex were also reported together with the terminal alkoxide complex of *p*-nitrobenzyl alcohol (Table 2) [113].

Two new bonding modes of aldehydes to zinc ions were described as a result of the studies on reactions of $Tp^{Cum,Me}Zn$-OH with aldehydes [109]. First α-hydroxy-alkoxide complex, derived from the hydrated aldehyde, was obtained for trichloroacetaldehyde (chloral) hydrate (Fig. 10e, Tables 2 and 3). A series of formylphenols attached to zinc as six-membered chelate rings was also studied (Fig. 10f, Tables 2 and 3). The aldehydes formed stable zinc complexes even in the presence of several good nitrogen donors. The authors suggested the protective role of the encapsulating pyrazolylborate ligands and the uncharged molecular nature of the complexes. The increase in the coordination number of zinc from four to five induced by the weakly coordinating aldehydes was mentioned as an indicator of a co-ligand (water?) coordination at the zinc ion, during the catalytic turnover of LADH [109].

Protonation/deprotonation of zinc-bound water molecules is a common feature of zinc enzymes and one of the crucial steps in the mechanism of action of zinc-dependent enzymes. The mechanism of action of alcohol dehydrogenase, which was considered to be different for a long time, has been recently reinvestigated and a zinc-bound water molecule was suggested to participate directly in this reaction (Fig. 5b [23,41,42,53,54]). Monometallic zinc complexes with N/S-chelating ligands and a single water molecule as a co-ligand are rather scarce. The only one example of such a neutral complex with $ZnNOS_2$ coordination was obtained with the use of sterically hindered tri-*tert*-butoxysilanethiol [92]. Seven ionic mono-zinc aqua complexes were obtained and structurally characterized with the use of chelating ligands. The first one was reported in 1998, when Weis and Vahrenkamp isolated penta-coordinated $Tp^{Pic,Me}Zn(H_2O)(PO_2(OC_6H_5)_2)$ [120]. The two co-ligands in the complex, i.e. water and diphenylphosphate were linked by a hydrogen bond (Fig. 10g, Tables 2 and 3) [120]. In 1999 Bergquist and Parkin reported a crystal structure of the zinc–aqua complex $\{[Tp^{tBu,Me}]Zn(OH_2)\}C_6F_5)_3B(OH)$ obtained by a protonation of a zinc-hydroxide complex $[Tp^{tBu,Me}]ZnOH$ by $(C_6F_5)_3B(OH_2)$ [121]. They observed that protonation resulted in a lengthening of the Zn–O bond by ca. 0.1 Å (Tables 2 and 3). The protonation was reversed by a treatment of $\{[Tp^{tBu,Me}]Zn(OH_2)\}^+$ with triethylamine [121]. Both aqua- and hydroxo-complexes of zinc with the ester substituted trispyrazolylborate ligand $Tp^{CO2Et,Me}$ which displayed internal hydrogen bonding were isolated and structurally characterized in 2002 [122]. Interestingly, the structure of the zinc complex, formed when the acetate salt was used for the synthesis of $Tp^{CO2Et,Me}Zn^+$, revealed two different molecules in the unit cell. One contained a pseudotetrahedral $Tp^{CO2Et,Me}$zinc–acetate complex while the second molecule in the cell was the five-coordinate aqua complex $[(Tp^{CO2Et,Me})Zn(OAc)(H_2O)]$, in which coordinated water was stabilized by two internal H-bonds (Fig. 10h, Tables 2 and 3) [122]. Finally three aqua and six terminal hydroxo-complexes were reported in a very comprehensive study by Vahrenkamp and coworkers [123] together with six examples of a new structural type, i.e. the OH-bridged dinuclear tripod–Zn complexes. Application of a new series of pyrazolylborates that bore 4-pyridyl or carboxamido substituents facilitated preparation of the $TpZn(OH_2)$ complexes. One is shown in Fig. 10i while the corresponding structural data are gathered in Tables 2 and 3 [123].

3.1.2.2. Amine-appended tetradentate tripodal ligands. Zinc complexes of amine-appended tetradentate tripodal ligands served as models of the influence of secondary hydrogen-bonding interactions on the chemistry of mononuclear zinc centers in the Berreau's research group [16]. The ligands are shown in Fig. 11. Nitrogen/sulfur-ligated zinc–methanol and zinc–*N*,*N*-dimethylformamide complexes relevant to substrate- and inhibitor-bound forms of LADH were generated with the use of a single internal hydrogen bond donor, i.e. *N*,*N*-bis-2-(methylthio)ethyl-*N*-(6-amino-2-pyridylmethyl)amine) (bmapa, Fig. 11) [124]. In Zn–bmapa complexes the amino group attached to the pirydyl ring formed a hydrogen bond with an additional ligand complexed to the mononuclear zinc center (Fig. 12a, Tables 2 and 3). The isolation of zinc complexes with bmapa/bmpa and formamide or sulfoxide ligands was also described [125]. The results indicated that the binding of a single formamide or sulfoxide ligand was competitive for an N/S-ligated zinc center in alcohol solutions as the complexes were isolated from methanol solutions, in which formamide/sulfoxide were only an addition [125].

Mononuclear zinc alkoxide species were successfully modeled by amine-appended tetradentate ligand systems containing one (bmnpa) or more (benpa, ebnpa) internal hydrogen-bond donors (Fig. 11). The preparation of a series of mononuclear and binuclear N_2S_2-ligated zinc–perchlorate, zinc–hydroxide, zinc–methoxide and zinc–aryloxide complexes was reported (Fig. 12b, c and d,

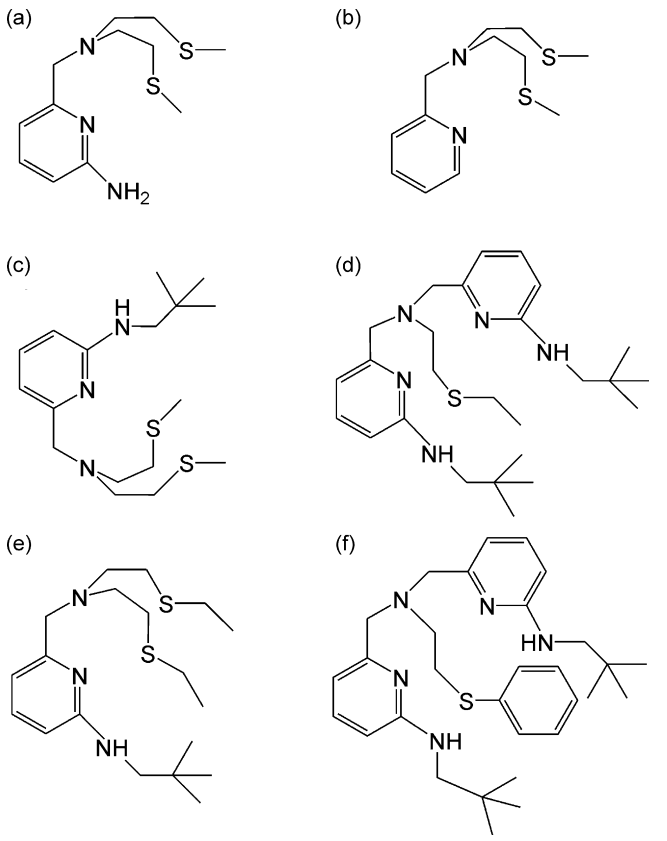

Fig. 11. The chelating N/S-ligands (II): (a) *N*,*N*-bis-2-(methylthio)ethyl-*N*-(6-amino-2-pyridylmethyl)amine) (bmapa) [124]; (b) *N*,*N*-bis-2-(methylthio) ethyl-*N*-(2-pyridylmethyl)amine) (bmpa) [125]; (c) *N*-bis-2-(methylthio)ethyl-*N*,*N*-bis(6-neopentylamino-2-pyridylmethyl)amine (benpa) [126]; (d) *N*-2-(ethylthio) ethyl-*N*,*N*-bis(6-neopentylamino-2-pyridylmethyl)amine (ebnpa) [127]; (e) (*N*,*N*-bis-2-(ethylthio)ethyl-*N*-(6-neopentylamino-2-pyridylmethyl)amine) (benpa) [128]; *N*-2-(phenylthio)ethyl-*N*,*N*-bis-((6-neopentylamino-2-pyridyl)methyl) amine (pbnpa) [132].

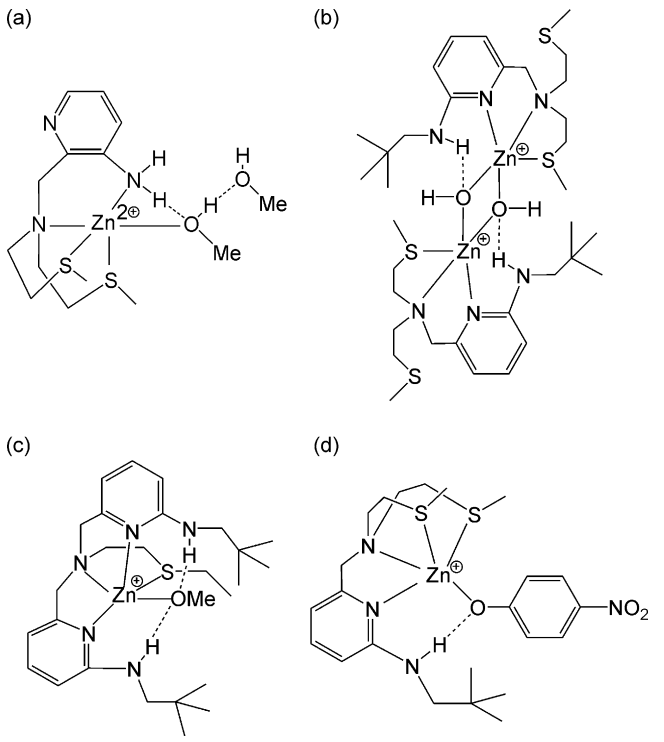

Fig. 12. Zinc complexes with the chelating N/S-ligands (II): (a) [(bmapa)(MeOH)Zn](ClO$_4$)·MeOH [124]; (b) {[(bmnpa)(OH)Zn](ClO$_4$)$_2$ [126]; (c) [(ebnpa)(OCH$_3$)Zn]ClO$_4$ [127]; (d) [(bmnpa)(*p*-OC$_6$H$_4$NO$_2$)Zn]ClO$_4$ [128].

Tables 2 and 3) [126–128]. In each complex, a hydrogen-bonding interaction was present between the zinc-bound hydroxide, methoxide or aryloxide oxygen atom and the secondary amine moiety of the supporting chelate ligand. The single internal hydrogen bond donor in hydroxide/methoxide as well as aryloxide complexes mimicked the proposed active site secondary hydrogen-bonding interaction involving Ser-48 and a zinc-bound alkoxide in the alcohol dehydrogenase [127,128]. The collective results for the aryloxide complexes pointed to the increase in the strength of the hydrogen-bonding interaction with the increasing basicity of the aryloxide moiety [128]. The hydrogen-bonding interactions in hydroxide and methoxide complexes nearly equivalent. However, the calculations of the solvent accessibility of the Zn–OCH$_3$ and Zn–OH units showed limited water access to the alkoxide oxygen in the methoxide complex contrary to the hydroxide species. Thus the authors concluded that in the studied system zinc alkoxide complex was stabilized with respect to the hydroxide derivative [127]. This finding, which was very important with regard to the mechanism of action of alcohol dehydrogenase was soon supported by the model studies of Chinese scientists who discovered that zinc(II)–alcohol complex is more easily deprotonated than zinc(II)–water [129]. This means that zinc(II)-coordinated alcohol has a lower pK_a than zinc(II)-coordinated water within the same molecule [129]. While the dehydrogenation reaction was not studied for bmnpa, benpa or ebnpa zinc complexes, it was later established that zinc methoxide species is a very active transesterification catalyst for formyl esters [130].

Apart from group 12 metals, the ligands described above were used for the synthesis of the first mononuclear nitrogen/sulfur-ligated Co(II) (also Cu(II) [131,132]) alkoxide complexes which were of relevance to the reactive intermediate observed for Co(II)-substituted liver alcohol dehydrogenase [133]. Preliminary EPR analysis of the two studied cobalt species indicated that both complexes were high-spin. Their paramagnetic ^{1}H NMR spectra were analyzed and several of the proton resonances were identified and assigned by selective deuteration. Similar hydrolytic stability for the Co(II) and Zn(II) methoxide derivatives was postulated and the same was hypothesized for Co(II)–OR species spectroscopically observable for Co(II)-containing LADH with regard to the proposed Zn(II)–OR intermediate in the catalytic cycle of the native enzyme [133].

3.1.2.3. Calixarenes. The ligation of water, ethanol and acetaldehyde with zinc was described for ternary zinc complexes of the calix[6]arene ligand possessing three imidazolyl arms (Fig. 13) [19,134–137]. The Zn–calix[6]arene complex contained a hydrophobic pocket and behaved as a selective molecular funnel for neutral guests that could bind to the metal center (Fig. 14a and b). The complexation of small organic molecules, which were deeply buried in the calixarene cavity, was stabilized by the ligand–calix[6]arene interactions similar to those reported for the LADH enzyme [136,137]. The Zn-ligated EtOH molecule was buried deeply inside the calixarene conic cavity (Fig. 14b). The Zn–O distance [1.984(5) Å] was similar to those reported for the four-coordinate ionic Zn–alcohol complexes (Table 2) and significantly shorter than those reported for the Zn–alcohol adducts in LADH (Table 2). The shortening was attributed by the authors to a different overall charge of the coordinated metal center in the model complex as compared to that in LADH [136]. The ethanol OH group pointed towards one of the OCH$_2$ImMe units with the relatively short O···O distance (2.86 Å, Fig. 14b, Table 3). Both the methyl and the methylene groups of the ethanol molecule were positioned in

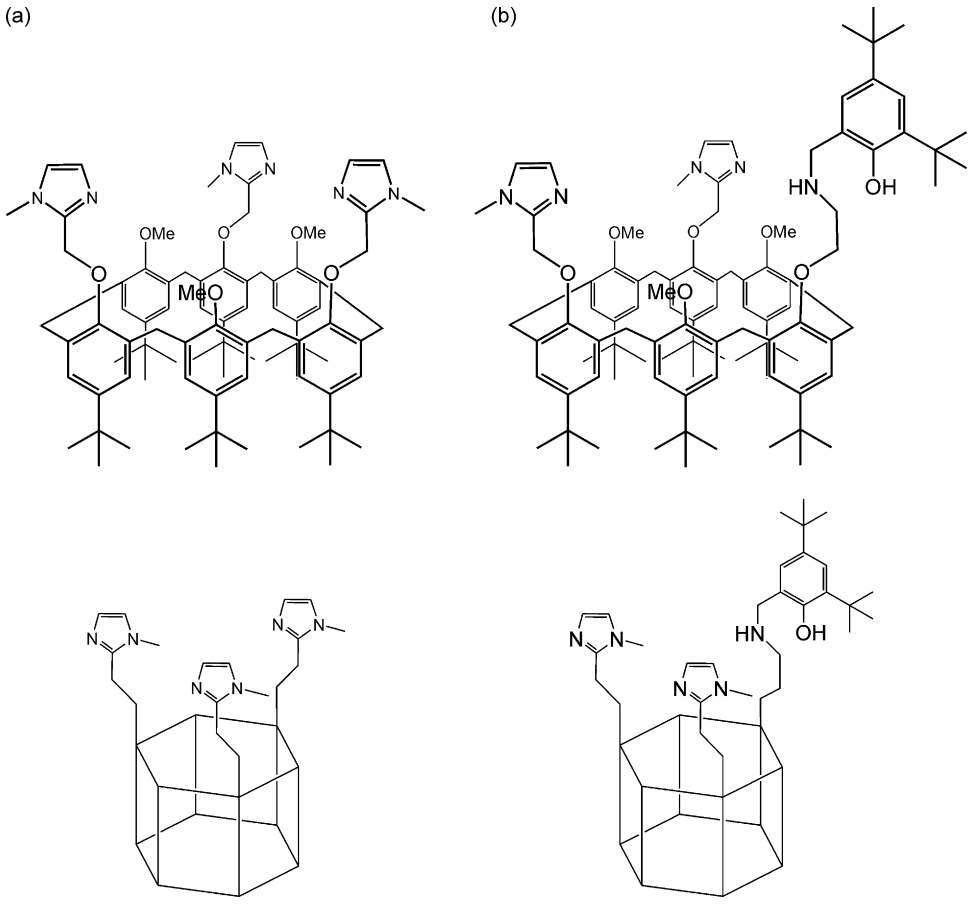

Fig. 13. The chelating N-ligands (III): (a) 5,11,17,23,29,35-Hexa-*tert*-butyl-37,39,41-trimethoxy-38,40,42-tris[(1-methyl-2-imidazolyl)methoxy]calix[6]arene; $X_6Et_3Imet_3$ [134,135,136]; (b) 5,11,17,23,29,35-Hexa-*tert*-butyl-37,39,41-trimethoxy-38-[2-[(3,5-di-*tert*-butyl-2-hydroxy)benzyl]-amino]-ethoxy]-40,42-bis[(1-methyl-2-imidazolyl) methoxy]calix[6]arene; Calix[6]N_3ArO [138]. The ligands are often presented schematically as shown in the lower part of the figure.

front of aromatic anisole rings with the perpendicular C···Ar distance of 3.67 and 3.82 Å, respectively. Such values indicated CH/π interactions between these moieties [136]. Formation of an adduct with acetaldehyde was initially observed by ^{1}H NMR spectroscopy when the aldehyde was added to a solution of the zinc–aqua complex in $CDCl_3$. The crystal structure of the first Zn–acetaldehyde complex revealed a similar stabilizing CH/π interaction of the aldehyde with the walls of the cavity. The Zn–O distance [1.882(8) Å] was significantly shorter than in the other previously reported zinc–aldehyde complexes (Table 2) reflecting a strongly acidic, dicationic zinc center [137].

Ligand exchange processes in the calix[6]arene cavity were quantitatively studied and equilibrium constants for binding of various small molecules were determined [135,137]; the affinity order for the LADH substrates was EtOH > MeCHO which is in agreement with the mechanism of LADH catalysis. The authors pointed to the relatively small differences between the binding constants, which were consistent with the reversibility of the LADH-catalyzed reaction [137].

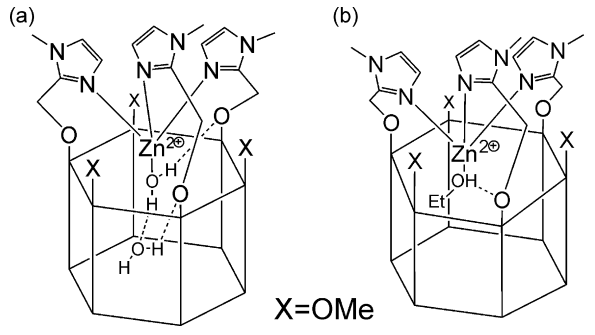

Fig. 14. Zinc complexes with the chelating N-ligands (III): (a) $(X_6Et_3Imet_3)(H_2O)Zn](ClO_4)_2{\cdot}H_2O$ [134]; (b) $[(X_6Et_3Imet_3)(EtOH)Zn](Cl_4)_2$ [136].

The coordination chemistry of zinc with the ligands based on calix[6]arenes that present two imidazole arms and an amino phenol moiety (Fig. 13) was explored and reported in 2005 [138]. Three different types of complexes were characterized including one dicationic with Zn^{2+} coordinated to the three nitrogen atoms and to the oxygen of the phenol group of the calix[6]ligand, a monocationic complex with deprotonated phenol group and finally neutral hydroxo-/chloride-complex. The simultaneous binding of two anionic donors decreases the Lewis acidity of the zinc ion within the complex [138].

3.1.2.4. Varia. In 1977 zinc and cobalt(II) complexes with tripodal tris(2-benzimidazylmethyl)amine were prepared and reported to possess a variety of stereochemistries, e.g. five-coordinate trigonal bipyramidal cations and four-coordinate anions. Interestingly, the blue cobalt complexes, i.e. $[Co(L)X]_2[CoX_4]$ could be readily converted to purple five-coordinate [Co(L)X]X complexes by recrystallization from a water-containing solvent. The electronic absorption spectra of four- and five-coordinate cobalt(II) species in acetone were studied [139].

In 1987 Kellogg and co-workers described the synthesis of zinc and cobalt(II) complexes with the use of chelating ligands designed to mimic the coordination environment of zinc in the

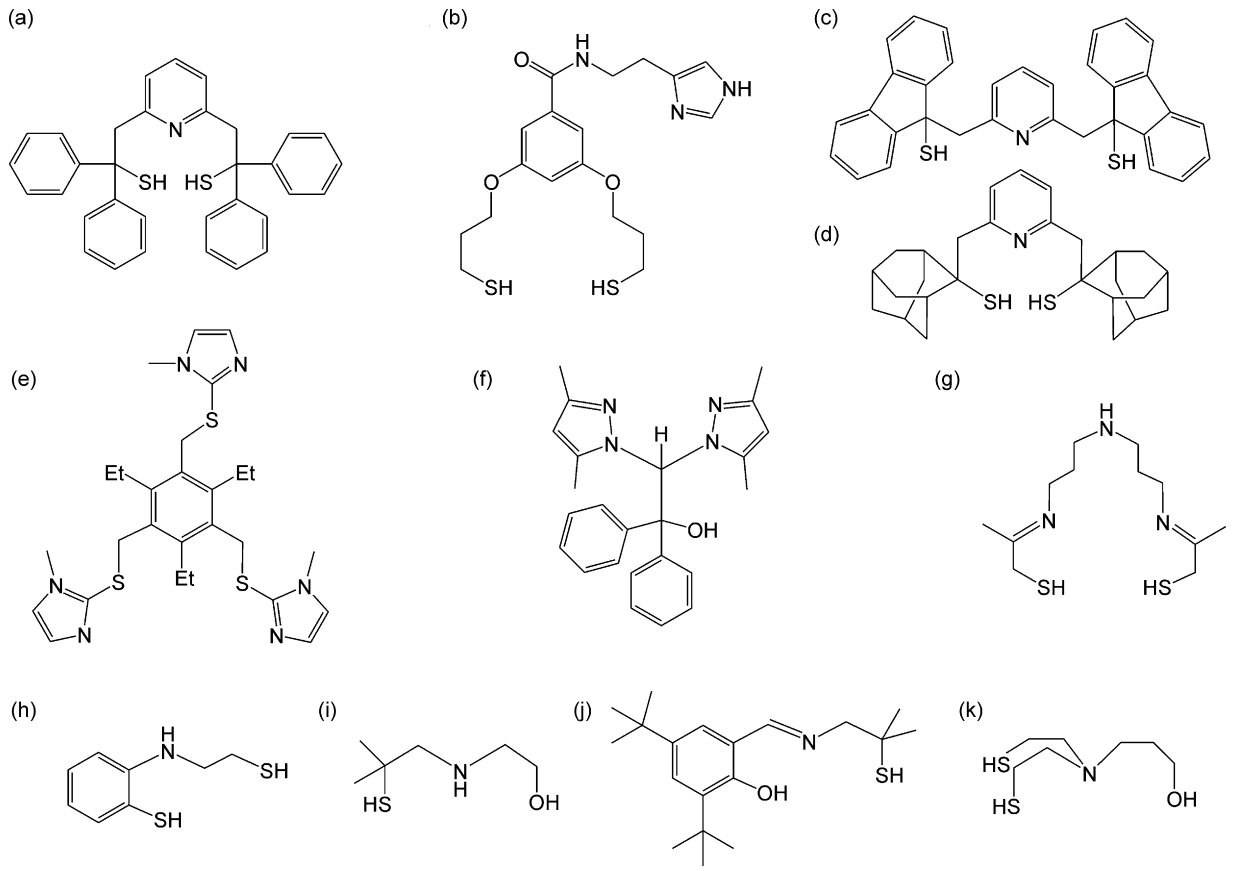

Fig. 15. The chelating S/N-ligands (IV): (a) 2,6-di-[(2′2′-diphenyl-2′-mercapto)ethyl]pyridine (DMEP) [140]; (b) 1-{N-[(imidazole-(4(5)′-yl)ethyl]amido-3,5-di-(3′-mercaptopropoxy)benzene [140]; (c) 2,6-di-[(2′-fluorenyl-2′-mercapto)ethyl]pyridine [140]; (d) 2,6-di-[(2′-adamantyl-2′-mercapto)ethyl]pyridine [142]; (e) 1,3,5-triethyl-2,4,6-tris[N-methyl-imidazole-2-yl-thiomethyl]benzene (TriMim) [145]; (f) bis(3,5-dimethylpyrazol-2-yl)diphenylmethanol (Bp^{Me}) [146]; (g) 1,2-dimethyl-3,7,1-triazatrideca-2,11-diene-1,13-dithiol ($L_{S2(Me)N3(Pr)}$) [147]; (h) N-(2-mercaptoethyl)-2-mercaptoaniline [148]; (i) mercaptoisobuthyl-hydroxyethylamine (H_2MIEH) [149]; (j) 2-mercaptoisobuthyliminomethyl-3,6-di-*tert*-buthylphenol [149]; 3-hydroxy-*N*,*N*-bis(2-mercaptoethyl)-propylamine [151].

LADH active site. Two different ligands were used in the study (Fig. 15a and b). Complexation of $Zn(NO_3)_2$ or $Co(NO_3)_2$ with 3,5-di-(3′-mercaptopropoxy)-N-(2′-imidazol-4(5)″-yl)ethyl) benzamide hydrochloride was accompanied by the release of three protons indicative of the formation of a neutral complex. The Zn^{2+} complex was amorphous, insoluble and probably oligomeric, but the non-crystalline Co^{2+} complex was slightly soluble. The electronic absorption spectrum of cobalt(II) complex of unknown structure was similar to the spectrum of LADH with Co(II) substituted at the active site. The same complex exhibited some catalytic activity in ketone reduction with BNA^+ [140]. Despite the fact that phenyl substituents crowded near the SH function, the zinc complex of the second ligand, i.e. the derivative of pyridinedithiol DMEP turned out to be dimeric even in diluted solutions (Fig. 16a) [140]. The studies were continued and greater steric hindrance was introduced into the dithiol compounds by incorporation of fluorene rings instead of phenyl groups in the vicinity of thiolate function (Fig. 15c). The authors did not obtain crystals suitable for X-ray analysis and suggested tricoordination on the basis of NMR spectra in solution [141]. One more ligand, synthesized with the intention to prepare biomimetic complexes of the catalytically active site of LADH, was described in 1996 and 1997 (Fig. 15d), but the crystal structure of its zinc complex was not determined [142–144].

Zinc- and relatively rare cadmium–aqua complexes of a new tris(imidazolyl)-based ligand, namely 1,3,5-triethyl-2,4,6-tris[N-methyl-imidazol-2-yl-thiomethyl]benzene (TriMim) (Fig. 15e) were synthesized and structurally characterized in 2004 [145]. They exhibited trigonal pyramidal metal ion coordination mode and hydrogen bonding between the metal-ligated water molecule and the non-coordinating counter ions (Fig. 16b). The differences in $Zn–OH_2$ distances reflected the H-bond accepting properties of the anions. The Zn–O distances in the two aqua complexes were significantly longer than those found in the calix[6]arene, Tp^R or Tm^R complexes (Tables 2 and 3) and closer to the Zn–O distances found in the enzyme [145].

The properties of a chelated *vs.* unchelated alkoxides complexed to the zinc ion in an environment very similar to that presented by tris(pyrazolyl)borate ligands (Fig. 15f) were compared by Hoffman and Carrano [146]. As a result of this study, it was concluded that nucleophilicity of a chelated zinc-bound alkoxide is lower than the nucleophilicity of monodentate alkoxide and definitely lower than that of zinc-bound thiolates [146].

Two penta-coordinate zinc complexes with imine and amine form of 1,2-dimethyl-3,7,1-triazatrideca-2,11-diene-1,13-dithiol (Fig. 15g) were obtained and structurally characterized [147]. The coordination environment of zinc in the complexes was different than in LADH, but both compounds crystallized as methanol solvates with methanol molecules hydrogen bonded to the thiolate sulfur. It was the fist example of thiolate–substrate interaction with the metal site approximating that of LADH (Fig. 16c). The OH···S interactions were investigated by means of solid-state FT-IR spectroscopy [147].

ZnS_2NX coordination was achieved with the polydonor ligand N-(2-mercaptoethyl)-2-mercaptoaniline (LH_2) featuring two SH functions, and one NH donor function (Fig. 15h) [148]. Its reaction with zinc salts yielded the 1:1 complex ZnL, however the structure analysis revealed a molecular tetramer structure. The addition of 2,2′-bipyridine co-ligand resulted in the formation of a

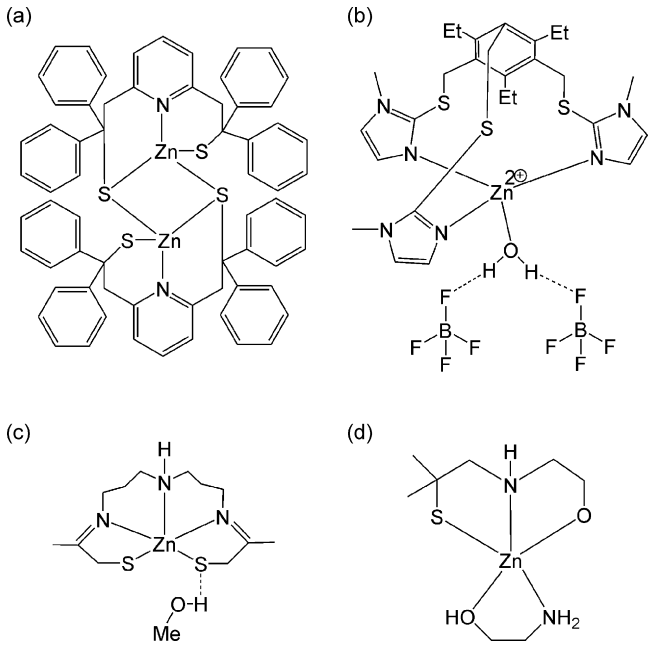

Fig. 16. Zinc complexes with the chelating S/N-ligands (IV): (a) [(DMEP)Zn] [140]; (b) [(TriMim)(H_2O)Zn](BF_4)$_2$ [145]; (c) [($L_{S2(Me)N3(Pr)}$)Zn]·MeOH [147]; (d) [(MIEH)($H_2N(CH_2)_2$)OH)Zn] [149].

monometallic complex ZnL(bipy) [148]. Five years later, three new tridentate ONS-ligands: mercaptoisobuthyl-hydroxyethylamine (Fig. 15i), mercaptoiso-buthyliminomethylphenol and its *tert*-butyl derivative (Fig. 15j) were used to synthesize zinc complexes with relevance to the active-site zinc of LADH [149]. Though homoleptic zinc complexes of these ligands exhibited higher nuclearities, when combined with hydroxyethylamine one of the ligands yielded a trigonal bipyramidal complex with ZnN_2O_2S coordination (Fig. 16d, Table 2). The next two produced mono-zinc complexes, with probably the same coordination patterns, in the presence of co-ligands such as, benzoylpyridine and phenylhydroxymethylpyridine (their crystal structures were not determined) [149]. Another similar ligand, i.e. bis(iminomethyl)-2,6-bis(mercaptoisobutyl)-4-methylphenol in a reaction with diethylzinc in the presence of alcohols yielded polynuclear complexes with bridging alkoxide ligands [(L)Zn_2(OR)] (R = CH_3, C_2H_5 and $CH_2C_6H_4CF_3$) and ZnN_2O_2S coordination [150].

The synthesis of a novel tripod 3-hydroxy-*N*,*N*-bis(2-mercaptoethyl)-propylamine (Fig. 15k), equipped with an unsymmetrical NOS_2 donor set, was reported in 2004 together with the preparation of its zinc and nickel complexes [151]. As could be expected, the lack of steric hindrance close to the sulfhydryl groups resulted in the formation of a tetranuclear zinc complex. The four thiolato-bridged metal centers exhibited distorted tetrahedral coordination geometry around the zinc(II) ions in an NS_3 coordination sphere. In the complex the hydroxyl functionalized ligand arm of the tripodal ligand remained uncoordinated [151].

3.1.3. Miscellaneous

A comprehensive study of zinc complexation by aldehydes was presented by Vahrenkamp et al. as a series of four papers [152–155]. The work provided some elementary information concerning zinc–substrate interactions within the active site of alcohol dehydrogenase. It was shown that aldehydes can be bound to zinc in the presence of water, although at the same time the excess water easily replaced zinc-bound aldehydes. Furthermore, alcohol and aldehyde ligands were found as the co-ligands in the same complex (Fig. 17a and b) [153]. Twelve heteroleptic zinc complexes with various substituted benzaldehydes and halides were structurally characterized and almost all compounds turned out to be molecular (neutral) complexes with tetrahedral geometry around the zinc ion (Fig. 17c). The only exception was the hexaaldehyde-zinc cation (Fig. 17d) [154]. Complexation of zinc with N,O chelating aldehyde and halide anions was also achieved (Fig. 17e and f) [155].

The synthesis of zinc complexes of amino acids and small cysteine-containing peptides in the context of the structural and functional roles of zinc in proteins, was described by Vahrenkamp in several papers, e.g. [156,157]. In the course of studies on the coordination modes of peptides with the two closely spaced cysteine residues the formation of a variety of highly stable zinc complexes in solution and in the solid state was observed. However, the simple coordination mode Zn-peptide was observed only in dilute solutions or in the heteroleptic complex with neocuproine. With the rising complex concentrations, the bridging tendency of the thiolate functions prevailed [156].

Very interesting model studies concerning the structural zinc-binding site of LADH were reported in 2008 [158]. Zinc coordination to the peptide analogues to residues 93–115 of horse-liver alcohol dehydrogenase (ADH) was examined by competitive binding and X-ray absorption fine structure analysis of the zinc ligands. The differences were observed in zinc coordination by the enzyme as compared to that by the model peptide. The authors suggested that even the "structural" zinc site in ADH is in a configuration that is energetically strained (relative to that of the model peptide) similar to that postulated for an active site of the enzyme [158].

3.2. Functional models of LADH active site

As described in the previous chapter, chemical models of the active site of LADH were usually aimed at reconstruction of the coordination environment around Zn. Although functional modeling of the active site is the most interesting aspect of bioinorganic chemistry, there are not many examples of functional, small molecule systems mimicking the catalytic action of alcohol dehydrogenase. Attempts to prepare monomeric zinc thiolates depend on the use of steric hindrance close to the donor sulfur atom to prevent its strong tendency to bridge two zinc ions. On the other hand, bulky ligands limit accessibility of zinc ion for substrate binding and the subsequent reaction with an oxidizing/reducing agent [159]. Close structural models usually did not exhibit any catalytic activity (e.g. [98,103]), thus the reported functional models often had little in common with the structure of the LADH active site.

3.2.1. Aldehyde/ketone reduction

The first functional model system was reported in 1971 [160]. Reduction of 1,10-phenanthroline-2-carboxaldehyde to 2-hydroxymethyl-1,10-phenanthroline by N-propyl-1,4-dihydronicotinamide in acetonitrile was catalyzed by zinc ions. The authors claimed that the catalytic efficiency of the zinc ion had to be significant since no reaction occurred in the absence of the metal ion. The studied 1,10-phenanthroline-2-carboxaldehyde was the first aldehyde reduced by the dihydronicotinamide in the non-enzymatic system (Fig. 18) [160]. Further studies carried out within the same reacting system indicated that proximity or direct coordination of the carbonyl group to the zinc ion is primarily responsible for the metal ion catalyzed reductions of chelating aldehydes [161]. A similar catalytic effect of zinc and magnesium cations was observed in the case of reduction of (E)-2-, (E)-3- and (E)-4-cinnamoylpyridines by 1,4-dihydropyridine derivatives. It was proved that the reduction was fastest when the metal ion was complexed in a chelating mode by the nitrogen and the oxygen sites of 2-cinnamoylpyridine [162].

An unusually fast, zinc-catalyzed reduction of pyridine-2-carbaldehyde by an alcohol dehydrogenase coenzyme model N′N′-

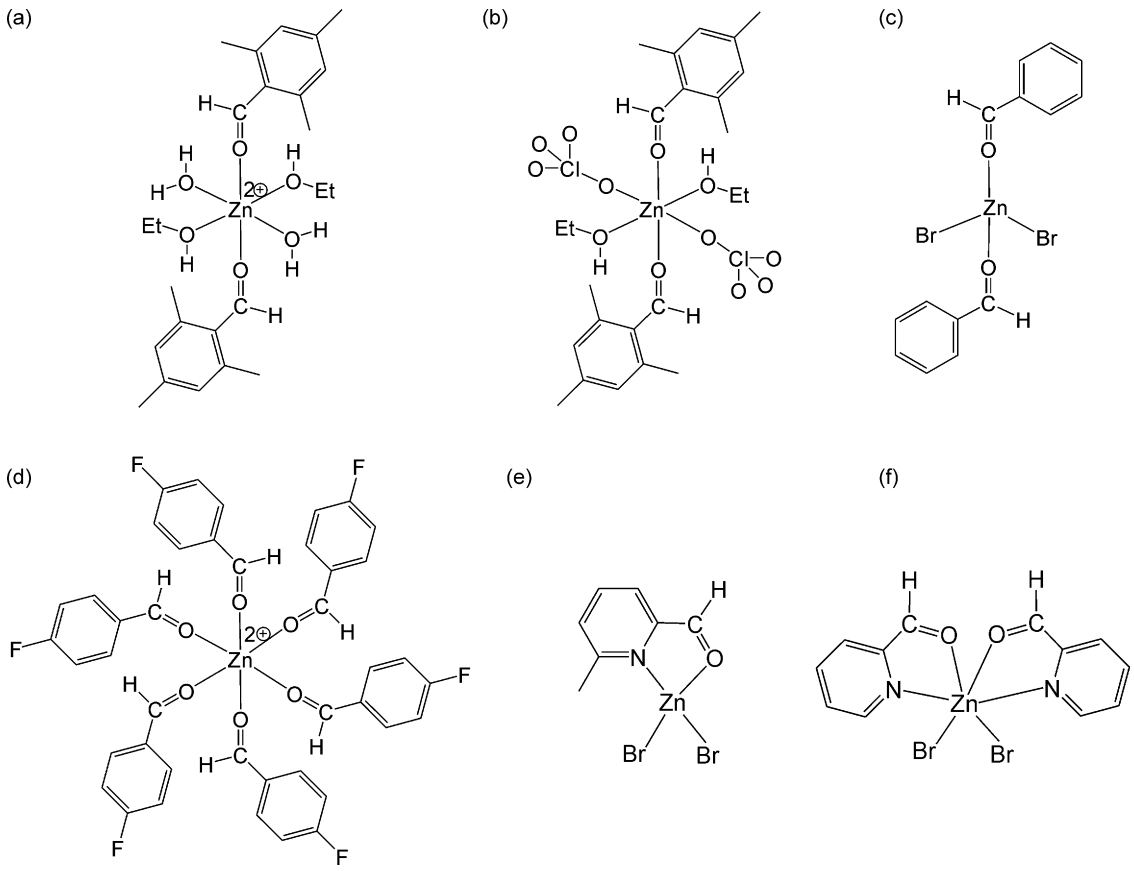

Fig. 17. Zinc complexes with aldehydes: (a) cation of $[(MesCHO)_2(EtOH)_2(H_2O)_2Zn](ClO_4)_2$ [153]; (b) $[(MesCHO)_2(EtOH)_2(ClO_4)_2Zn]$ [153]; (c) $[(C_6H_5CHO)_2Br_2Zn]$ [154]; (d) cation of $[(p\text{-}FC_6H_4CHO)_6Zn]$ $[Zn_2Br_6]$ [154]; (e) $[(PicCHO)Br_2Zn]$ [155]: (f) $[(PyCHO)_2Br_2Zn]$ [155].

diethyl-N-benzyl-1,4-dihydronicotinamide in acetonitrile was described in 1979 [163]. The kinetic differences between two NADH analogues were reported together with the unusually high specificity of N′N′-diethyl-N-benzyl-1,4-dihydronicotinamide towards one of the isomeric forms of the substrate. In the presence of anhydrous zinc bromide among the three pyridinecarbaldehyde substrates only pyridine-2-carbaldehyde was reduced. In the absence of a zinc compound the reaction was extremely slow [163].

Further systematic studies on the reduction of carbonyl function by NAD(P)H model compounds, carried out with the use of "naked" metal ions as catalysts, led to the unexpected conclusion that a mechanism of catalysis was different from the mechanism of zinc-catalyzed reaction in LADH. It was observed that bivalent ions such as Mg^{2+} and Zn^{2+} formed a complex with NADH models instead of carbonyl substrates [164,165]. A sandwich structure of the transition state ternary complex was suggested to be responsible for the catalytic effect ([165,166] and the papers cited therein). However in their contradictory reports Fukuzumi et al. proved that the reducing ability of NAD(P)H analogues was lowered by the complexation of metal ions, and the reaction of hydride transfer was decelerated [167,168]. Thus the role of metal ion seems to be at least dual as it participates in the formation of a complex and very probably takes part in the stabilization of the anionic transition state of the carbonyl compound [165].

The influence of the metal ion on the reducing power of NADH analogue, N-benzyl-1,4-dihydronicotinamide (BNAH) was presented in an elegant work of Ishitani et al. [169]. The acidity of the carbamoyl group of BNAH increases by coordination to the ruthenium(II) or rhenium(I) complex. In consequence, the deprotonated BNAH-Ru(II) and Re(I) complexes had much stronger hydride-donating abilities and were oxidized at more negative potentials than "free" BNAH. Additionally the adduct of NAD^+ analogue, i.e. N-benzylnicotinamide chloride (BNA^+) and the ruthenium complex was isolated and its crystal structure successfully determined [169].

3.2.2. Alcohol oxidation

Contrary to the reduction of the carbonyl group which is spontaneous, the opposite reaction, i.e. hydride transfer from alcohols to pyridinium salts such as NAD^+ is thermodynamically unfavorable, and that makes it a difficult subject for the studies.

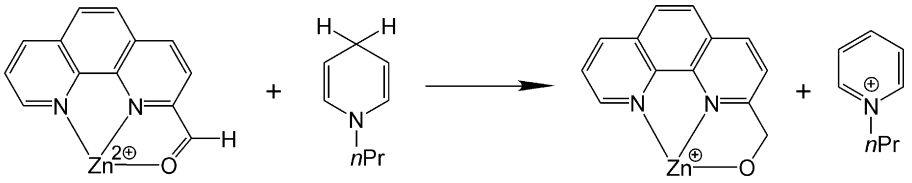

Fig. 18. Reduction of 1,10-phenanthroline-2-carboxaldehyde to the respective alcohol by N-n-propyl-1,4-dihydronicotinamide in the presence of zinc ions. According to [160].

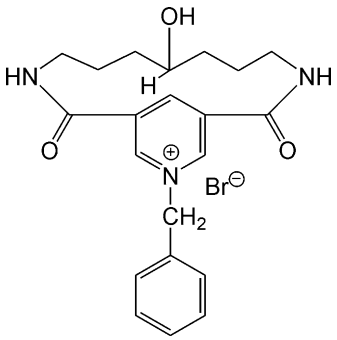

Fig. 19. A model for the intramolecular hydride transfer: 15-benzyl-2,12-dioxo-7-hydroxy-3,11,15-triazoniumbicyclo-[11.3.11 heptadeca-1(17),13,15-triene bromide. According to [172].

The equilibrium constant for the reaction:

$$CH_3CH_2OH + NAD^+ = CH_3CHO + NADH + H^+$$

was reported by Bäcklin as 6.46×10^{-12} [170] and Burton as $\sim 10^{-12}$ [171].

One of the early attempts to achieve non-enzymatic oxidation of an alcohol to a ketone by pyridinium salt was described in 1972 [172]. Studies on a rigid model system were reported in which intramolecular hydride transfer was possible only to position 4 of the pyridinium ring (Fig. 19). Despite close approximation of the enzyme situation and treatment of the compound with the various basic catalysts such as, sodium hydroxide in aqueous solution, sodium hydride, lithium bis(trimethylsilyl)amide, potassium *tert*-butoxide, *tert*-butyl-lithium, and aluminum isopropoxide in the strictly anhydrous conditions, intramolecular hydride transfer was not observed in the system. Overman ascribed this inertness to the improper orientation of the reacting groups for the hydride transfer [172].

Interesting comparative studies on the influence of zinc acidity and its coordination environment on the hydride transfer reaction were presented in 1992 [173]. Among the several macrocyclic polyamine zinc complexes that had been tested as functional LADH mimics, only one exhibited measurable catalytic activity. Reaction of BNA^+ with isopropyl alcohol in the presence of (1,5,9-triazacyclododecane)$Zn(OH)^+$ led to the formation of the 1,4-adduct BNAH with 17% yield. 1,6-Adduct was detected as the minor product (Fig. 20). Other similar Zn(II) species did not act as the catalysts. The authors explained this special catalytic efficiency of (1,5,9-triazacyclododecane)$Zn(OH)^+$ by the relatively high acidity of water in this system, together with the largest space available for the reaction [173,174].

Another example of functional LADH modeling with a zinc(II) complex was described almost 10 years later by Vahrenkamp [175]. 2-Propanol present within the complex [tris(3-cumenyl-5-methylpyrazolyl)borate]Zn-$OCHMe_2$ was oxidized by BNA(Cl) with the formation of BNAH (14% yield) $(BNA)_2$ (1% yield), acetone and [tris(3-cumenyl-5-methylpyrazolyl)borate]Zn-Cl. The

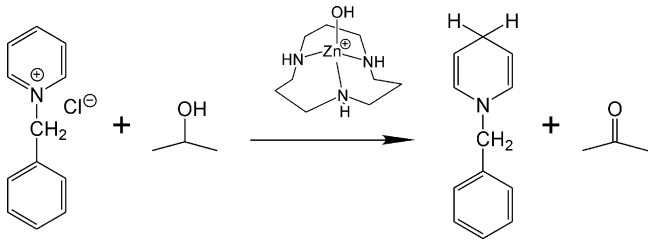

Fig. 20. Oxidation of 2-propanol by N-benzylnicotinamide chloride in the presence of a model zinc complex: {[12]aneN$_3$(OH)Zn}(CF$_3$SO$_3$). According to [173].

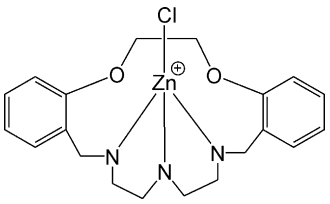

Fig. 21. An open-sphere zinc complex with macrocyclic ligand 1,12,15-triaza-3,4:9,10-dibenzo-5,8-dioxacyclo-heptadecane. The complex exhibited some catalytic activity in the reaction of oxidation of isopropanol with BNA(Cl) [176].

described system was a little bit more efficient compared to the previous one [173,175] although still much worse than the alcohol dehydrogenase.

The catalytic activity was also found for $Tm^{Cum}Zn^+$ complex, however the efficiency was not improved; the reaction took several hours to go to completion at 100 °C, but no acetone was formed in the absence of the studied zinc compound [103].

The close structural models of the LADH–zinc complexes with bis(1-*o*-anisole-2-mercaptoimidazolyl)(pyrazolyl)borate ligands showed no or very low catalytic efficiency. The results obtained for the same model system, namely (BNA(Cl)/2-propanol or BNAH/*p*-nitrobenzaldehyde were very poor because after 24 h of heating a 2–3% yield of acetone and traces of *p*-nitrobenzyl alcohol were obtained. It should be underlined that the applied complexes were the closest structural models of the enzyme available at that time [108]. A better catalytic efficiency was described by the same research group for an open-sphere zinc complex with macrocyclic ligand 1,12,15-triaza-3,4:9,10-dibenzo-5,8-dioxacyclohepta-decane. The complex, which is structurally different from the LADH active site, was catalytically active in the oxidation of alcohol. The reaction was slow and required large amounts of the complex (Fig. 21) [176].

Hydride transfer to the NAD^+ model, 10-methylacridinium perchlorate was shown for the solutions containing the zinc-hydroxide complex $[Tp^{But,Me}]ZnOH$ in methanol, ethanol, and isopropanol. Disappointingly, deuterium labeling studies demonstrated that the source of the hydride was not the alcohol but, the B-H group of the $[Tp^{But,Me}]$ ligand [177].

4. Summary

In conclusion chemists are presently able to attach the molecules of water, alcohols and aldehydes to the zinc ion together with the variety of N- and S-ligands, and the properties of such arrangements can be described in great detail including the precise distances between atoms. Unfortunately we are still unable to approach the catalytic efficiency of the LADH. The mechanism of the reaction of hydride transfer between the NADH analogues and carbonyl substrates, when studied in a test tube, seems to be different from that of the enzyme. Moreover, contradictory results are obtained concerning the influence of a metal ion on the reaction rate. Based on the architecture of the enzyme, we managed to build the interior of this natural nanoreactor, but the "breathing" walls are still missing.

Studies on simple coordination bioinorganic models are a useful source of information about the properties of metal ions and their ligands, but it still seems questionable whether this approach to reproduce the enzyme function has a chance of success, at least in the case of LADH. The reaction of alcohol oxidation by NAD^+ is thermodynamically unfavorable and in a bulk reaction mixture the equilibrium is established at very low aldehyde concentrations. The situation seems to be reversed in the hydrophobic cavity of the enzyme by the concerted action of zinc, H-bond and hydrophobic interactions that position NAD^+ for the hydride transfer, a net of

H-bonds that transport the protons in the desired direction, and finally movements of the whole protein molecule.

Acknowledgement

The support of the Polish Ministry of Science and Higher Education is gratefully acknowledged (Grant No. N N204 274835).

References

[1] D.S. Auld, Biometals 14 (2001) 271.
[2] W. Maret, J. Trace Elements Med. Biol. 19 (2005) 7.
[3] K. Patel, A. Kumar, S. Durani, Biochim. Biophys. Acta 1774 (2007) 1247.
[4] B.L. Vallee, D.S. Auld, Proc. Natl. Acad. Sci. U.S.A. 87 (1990) 220.
[5] (a) A. Kilhstein-Vardi, M. Glick, H.M. Greenblatt, A. Goldblum, G. Shoham, Acta Crystallogr. D59 (2003) 323;
(b) A.C. English, C.R. Groom, R.E. Hubbard, Protein Eng. 14 (2001) 47;
(c) Z. Fisher, J.A. Hernandez Prada, C. Tu, D. Duda, C. Yoshioka, H. An, L. Govindasamy, D.N. Silverman, R. McKenna, Biochemistry 44 (2005) 1097;
(d) S. Iyer, R. Visse, H. Nagase, K. Ravi Acharya, J. Mol. Biol. 362 (2006) 78;
(e) H.W. Park, S.R. Boduluri, J.F. Moomaw, P.J. Casey, L.S. Beese, Science 275 (1997) 1800;
(f) B.W. Poland, M.-Q. Xu, F.A. Quiocho, J. Biol. Chem. 275 (2000) 16408;
(g) J.E. Guy, M.N. Isupov, J.A. Littlechild, J. Mol. Biol. 331 (2003) 1041;
(h) X. Cheng, X. Zhang, J.W. Pflugrath, F.W. Studier, Proc. Natl. Acad. Sci. U.S.A. 91 (1994) 4034;
(i) D. Jozic, G. Bourenkov, N.-H. Lim, R. Visse, H. Nagase, W. Bode, K. Maskos, J. Biol. Chem. 280 (2005) 9578;
(j) M.S. Niederhut, B.J. Gibbons, S. Perez-Miller, T.D. Hurley, Protein Sci. 10 (2001) 697;
(k) S. Xiang, S.A. Short, R. Wolfenden, C.W. Carter Jr., Biochemistry 35 (1996) 1335;
(l) G. Auerbach, A. Herrmann, A. Bracher, G. Bader, M. Gütlich, M. Fischer, M. Neukammi, M. Garrido-Franco, J. Richardson, H. Nar, R. Huber, A. Bacher, Proc. Nat. Acad. Sci. U.S.A. 97 (2000) 13567;
(m) P.T. Erskine, R. Newbold, A.A. Brindley, S.P. Wood, P.M. Shoolingin-Jordan, M.J. Warren, J.B. Cooper, J. Mol. Biol. 312 (2001) 133.
[6] A. Messerschmidt, W. Bode, M. Cygler (Eds.), Handbook of Metalloproteins, vol. 3, John Wiley & Sons, Ltd., Chichester, UK, 2004, p. 1.
[7] B.L. Vallee, D.S. Auld, Acc. Chem. Res. 23 (1993) 543.
[8] I.L. Alberts, K. Nadassy, S.J. Wodak, Protein Sci. 7 (1998) 1700.
[9] J.C. Ebert, R.B. Altman, Protein Sci. 17 (2008) 54.
[10] F.H. Allen, Acta Crystallogr. B58 (2002) 380; Cambridge Structural Database, Version 5.30 of November 2008, update 4 September (2009).
[11] G. Parkin, Chem. Rev. 104 (2004) 699.
[12] H. Vahrenkamp, Acc. Chem. Res. 32 (1999) 589.
[13] A. Otero, J. Fernández-Baeza, A. Antiñolo, J. Tejeda, A. Lara-Sánchez, Dalton Trans. (2004) 1499.
[14] G. Parkin, Chem. Commun. (2000) 1971.
[15] J. Weston, Chem. Rev. 105 (2005) 2151.
[16] L.M. Berreau, Eur. J. Inorg. Chem. (2006) 273.
[17] L.M. Berreau, Comment. Inorg. Chem. 28 (2007) 123.
[18] G. Parkin, New J. Chem. 31 (2007) 1996.
[19] D. Coquière, S. Le Gac, U. Darbost, O. Sénèque, I. Jabin, O. Reinaud, Org. Biomol. Chem. 7 (2009) 2485.
[20] G. Duester, J. Farres, M.R. Felder, R.S. Holmes, J.-O. Höög, X. Pares, B.V. Plapp, S.-J. Yin, H. Jörnvall, Biochem. Pharmacol. 58 (1999) 389.
[21] J.-O. Höög, J.J. Hedberg, P. Strömberg, S. Svensson, J. Biomed. Sci. 8 (2001) 71.
[22] C.A. Staab, M. Hellgren, J.-O. Höög, Cell. Mol. Life Sci. 65 (2008) 3950.
[23] R. Meijers, E. Cedergren-Zeppezauer, in: A. Messerschmidt, W. Bode, M. Cygler (Eds.), Handbook of Metalloproteins, vol. 3, John Wiley & Sons, Ltd., Chichester, UK, 2004, p. 5.
[24] C.S. Lieber, Alcohol Clin. Exp. Res. 23 (1999) 991.
[25] R.A. King, J.I. Rotter, A.G. Motulsky (Eds.), The Genetic Basis of Common Diseases, 2 ed., Oxford University Press, UK, 2002.
[26] B. Persson, J.S. Zigler, H. Jörnvall, Eur. J. Biochem. 226 (1994) 15.
[27] B. Persson, J. Hedlund, H. Jörnvall, Cell. Mol. Life Sci. 65 (2008) 3879.
[28] G. Pettersson, Crit. Rev. Biochem. Mol. Biol. 21 (1987) 349.
[29] S. Al-Karadaghi, E.S. Cedergren-Zeppezauer, S.K. Hovmöller, P. Kyriakos, H. Terri, Z. Dauter, K. Wilson, Acta Crystallogr. D 50 (1994) 793, RCSB PDB entry 2OHX http://pdb.rcsb.org/pdb/home/home.do.
[30] Y. Pocker, Chem. Biol. Interact. 130–132 (2001) 383.
[31] H. Theorell, B. Chance, Acta Chem. Scand. 5 (1951) 1127.
[32] C.-I. Brånden, H. Eklund, B. Nordstrom, T. Boiwe, G. Soderlund, E. Zeppezauer, I. Ohlsson, A. Akeson, Proc. Natl. Acad. Sci. U.S.A. 70 (1973) 2439.
[33] S. Rao, M. Rossmann, J. Mol. Biol. 76 (1973) 241.
[34] S. Ramaswamy, H. Eklund, B.V. Plapp, Biochemistry 33 (1994) 5230, RCSB PDB entry 1HLD http://pdb.rcsb.org/pdb/home/home.do.
[35] H. Eklund, S. Ramaswamy, Cell. Mol. Life Sci. 65 (2008) 3907.
[36] L. Esposito, I. Bruno, F. Sica, C.A. Raia, A. Giordano, M. Rossi, L. Mazzarella, A. Zagari, Biochemistry 42 (2003) 14397.
[37] B.J. Bahnson, T.D. Colby, J.K. Chin, B.M. Goldstein, J.P. Klinman, Proc. Natl. Acad. Sci. U.S.A. 94 (1997) 12797.
[38] J.K. Rubach, B.V. Plapp, Biochemistry 42 (2003) 2907.
[39] C.I. Branden, H. Eklund, Ciba Found. Symp. (1977) 63.
[40] F. Colonna-Cesari, D. Perahia, M. Karplus, H. Eklund, C.I. Branden, O. Tapia, J. Biol. Chem. 261 (1986) 15273.
[41] E.G. Kovaleva, B.V. Plapp, Biochemistry 44 (2005) 12797.
[42] (a) B.V. Plapp, D.C. Sogin, R.T. Dworschack, D.P. Bohlken, C. Woenckhaus, Biochemistry 25 (1986) 5396;
(b) V. Chandra Sekhar, B.V. Plapp, Biochemistry 27 (1988) 5082;
(c) V. Chandra Sekhar, B.V. Plapp, Biochemistry 29 (1990) 4289;
(d) L.A. LeBrun, D.-H. Park, S. Ramaswamy, B.V. Plapp, Biochemistry 43 (2004) 3014.
[43] H.A. Charlier Jr., B.V. Plapp, J. Biol. Chem. 275 (2000) 11569.
[44] H.-L. Liu, Y. Ho, C.-M. Hsu, Chem. Phys. Lett. 372 (2003) 249.
[45] H.-L. Liu, Y. Ho, C.-M. Hsu, J. Biomed. Sci. 10 (2003) 302.
[46] H.-W. Adolph, P. Zwart, R. Meijers, I. Hubatsch, M. Kiefer, V. Lamzin, E. Cedergren-Zeppezauer, Biochemistry 39 (2000) 12885.
[47] H.W. Adolph, P. Maurer, H. Schneider-Bernlohr, C. Sartorius, M. Zeppezauer, Eur. J. Biochem. 201 (1991) 615.
[48] T.H. Venkataramaiah, B.V. Plapp, J. Biol. Chem. 278 (2003) 36699.
[49] M.F. Dunn, H. Dietrich, A.K.H. MacGibbon, S.C. Koerber, M. Zeppezauer, Biochemistry 21 (1982) 354.
[50] D.S. Auld, T. Bergman, Cell. Mol. Life Sci. 65 (2008) 3961.
[51] B.L. Vallee, D.S. Auld, Proc. Nat. Acad. Sci. U.S.A. 87 (1990) 220.
[52] B.R. Bobsein, R.J. Myers, J. Biol. Chem. 256 (1981) 5313.
[53] R. Meijers, R.J. Morris, H.W. Adolph, A. Merli, V.S. Lamzin, E.S. Cedergren-Zeppezauer, J. Biol. Chem. 276 (2001) 9316.
[54] R. Meijers, H.-W. Adolph, Z. Dauter, K.S. Wilson, V.S. Lamzin, E.S. Cedergren-Zeppezauer, Biochemistry 46 (2007) 5446.
[55] M. Makinen, W. Maret, M.B. Yim, Proc. Natl. Acad. Sci. U.S.A. 80 (1983) 2584.
[56] O. Kleifeld, L. Rulíšek, O. Bogin, A. Frenkel, Z. Havlas, Y. Burstein, I. Sagi, Biochemistry 43 (2004) 7151.
[57] U. Ryde, Protein Sci. 4 (1995) 1124.
[58] P.C. Sanghani, H. Robinson, W.F. Bosron, T.D. Hurley, Biochemistry 41 (2002) 10778.
[59] P.J. Baker, K. Linda Britton, M. Fisher, J. Esclapez, C. Pire, M.J. Bonete, J. Ferrer, D.W. Rice, Proc. Natl. Acad. Sci. U.S.A. 106 (2009) 779.
[60] J. Schmidt, J. Chen, M. DeTraglia, D. Minkel, J.T. McFarland, J. Am. Chem. Soc. 101 (1979) 3634.
[61] J. Kvassman, J.G. Pettersson, Eur. J. Biochem. 103 (1980) 557.
[62] J. Kvassman, G. Pettersson, Eur. J. Biochem. 103 (1980) 565.
[63] P.K. Agarwal, S.P. Webb, S. Hammes-Schiffer, J. Am. Chem. Soc. 122 (2000) 4803.
[64] Z.D. Nagel, J.P. Klinman, Chem. Rev. 106 (2006) 3095.
[65] Z.-X. Liang, J.P. Klinman, Curr. Opin. Struct. Biol. 14 (2004) 648.
[66] G.T.M. Henehan, N.J. Oppenheimer, Biochemistry 32 (1993) 735.
[67] B.V. Plapp, R.L. Brookes, J.D. Shore, J. Biol. Chem. 248 (1973) 3470.
[68] C.L. Stone, M.B. Jipping, K. Owusu-Dekyi, T.D. Hurley, T.-K. Li, W.F. Bosron, Biochemistry 38 (1999) 5829.
[69] K.A. McCall, C.-C. Huang, C.A. Fierke, J. Nutr. 130 (2000) 1437S.
[70] W. Kaim, B. Schwederski, Bioinorganic Chemistry: Inorganic Elements in the Chemistry of Life, Wiley, 1994.
[71] I.G. Dance, Polyhedron 5 (1986) 1037.
[72] P.J. Blower, J.R. Dilworth, Coord. Chem. Rev. 76 (1987) 121.
[73] J.R. Dilworth, J. Hu, Adv. Inorg. Chem. 40 (1993) 411.
[74] D.T. Corwin Jr., R. Fikar, S.A. Koch, Inorg. Chem. 26 (1987) 3080.
[75] B. Müller, A. Schneider, M. Tesmer, H. Vahrenkamp, Inorg. Chem. 38 (1999) 1900.
[76] D.T. Corwin Jr., E.S. Gruff, S.A. Koch, J. Chem. Soc. Chem. Commun. (1987) 966.
[77] D.T. Corwin Jr., S.A. Koch, Inorg. Chem. 27 (1988) 493.
[78] E.S. Gruff, S.A. Koch, J. Am. Chem. Soc. 111 (1989) 8762.
[79] M. Bochmann, K.J. Webb, M.B. Hursthouse, M. Mazid, J. Chem. Soc. Chem. Commun. (1991) 1735.
[80] M. Bochmann, G.C. Bwembya, R. Grinter, A.K. Powell, K.J. Webb, M.B. Hursthouse, K.M. Abdul Malik, M.A. Mazid, Inorg. Chem. 33 (1994) 2290.
[81] M. Bochmann, G. Bwembya, R. Grinter, J. Lu, K.J. Webb, D.J. Williamson, Inorg. Chem. 32 (1993) 532.
[82] J.J. Ellison, P.P. Power, Inorg. Chem. 33 (1994) 4231.
[83] R.M. Catala, M.E. Colsa, D. Cruz-Garritz, H. Torrens, J.L. Brianso, J.E. Piniella, G. Germain, Trans. Met. Chem. 12 (1987) 197.
[84] J.R. Dilworth, J. Hu, Adv. Inorg. Chem. 40 (1994) 411.
[85] M. Wojnowska, W. Wojnowski, Z. Allg. Anorg. Chem. 403 (1974) 179.
[86] B. Becker, K. Radacki, W. Wojnowski, J. Organomet. Chem. 521 (1996) 39.
[87] B. Becker, A. Dołęga, A. Konitz, W. Wojnowski, Polyhedron 20 (2001) 949.
[88] B. Becker, A. Pladzyk, A. Konitz, W. Wojnowski, Appl. Organometal. Chem. 16 (2002) 517.
[89] A. Kropidłowska, J. Chojnacki, B. Becker, J. Inorg. Biochem. 101 (2007) 578.
[90] A. Dołęga, B. Becker, J. Chojnacki, A. Konitz, W. Wojnowski, Inorg. Chim. Acta 357 (2004) 461.
[91] A. Dołęga, M. Wieczerzak, K. Baranowska, Acta Crystallogr. Sect. E Struct. Rep. Online 63 (2007) m1774.
[92] A. Dołęga, A. Pladzyk, K. Baranowska, M. Wieczerzak, Inorg. Chem. Commun. 11 (2008) 847.
[93] A. Dołęga, K. Baranowska, A. Pladzyk, K. Majcher, Acta. Crystallogr C64 (2008) m259.
[94] A. Dołęga, K. Baranowska, D. Gudat, A. Herman, J. Stangret, A. Konitz, M. Śmiechowski, S. Godlewska, Eur. J. Inorg. Chem. (2009) 3644.

[95] A. Dołęga, A. Pladzyk, K. Baranowska, J. Jezierska, Inorg. Chim. Acta 362 (2009) 5085.
[96] A. Dołęga, K. Baranowska, J. Gajda, S. Kaźmierski, M. Potrzebowski, Inorg. Chim. Acta 360 (2007) 2973.
[97] A. Dołęga, A.M. Walewski, Magn. Reson. Chem. 45 (2007) 410.
[98] N.J. Curtis, R.S. Brown, Can. J. Chem. 59 (1981) 65.
[99] S. Trofimenko, Chem. Rev. 72 (1972) 497.
[100] S. Trofimenko, Chem. Rev. 93 (1993) 943.
[101] M. Garner, J. Reglinski, I. Cassidy, M.D. Spicer, A.R. Kennedy, J. Chem. Soc. Chem. Commun. (1996) 1975.
[102] C. Kimblin, B.M. Bridgewater, D.G. Churchill, G. Parkin, Chem. Commun. (1999) 2301.
[103] M. Tesmer, M. Shu, H. Vahrenkamp, Inorg. Chem. 40 (2001) 4022.
[104] Inorg. Chim. Acta 362 (2009) 4659.
[105] M. Rombach, J. Seebacher, M. Ji, G. Zhang, G. He, M.M. Ibrahim, B. Benkmil, H. Vahrenkamp, Inorg. Chem. 45 (2006) 4571.
[106] U. Brand, M. Rombach, J. Seebacher, H. Vahrenkamp, Inorg. Chem. 40 (2001) 6151.
[107] J. Seebacher, M. Shu, H. Vahrenkamp, Chem. Commun. (2001) 1026.
[108] M. Shu, R. Walz, B. Wu, J. Seebacher, H. Vahrenkamp, Eur. J. Inorg. Chem. (2003) 2502.
[109] R. Walz, M. Ruf, H. Vahrenkamp, Eur. J. Inorg. Chem. (2001) 139.
[110] C. Kimblin, T. Hascall, G. Parkin, Inorg. Chem. 36 (1997) 5680.
[111] C. Kimblin, B.M. Bridgewater, D.G. Churchill, T. Hascall, G. Parkin, Inorg. Chem. 39 (2000) 4240.
[112] J.K. Rubach, B.V. Plapp, Biochemistry 41 (2002) 15770.
[113] M.M. Ibrahim, M. Shu, H. Vahrenkamp, Eur. J. Inorg. Chem. (2005) 1388.
[114] R. Walz, K. Weis, M. Ruf, H. Vahrenkamp, Chem. Ber. 130 (1997) 975.
[115] C. Bergquist, G. Parkin, Inorg. Chem. 38 (1999) 422.
[116] H. Brombacher, H. Vahrenkamp, Inorg. Chem. 43 (2004) 6042.
[117] C. Bergquist, H. Storrie, L. Koutcher, B.M. Bridgewater, R.A. Friesner, G. Parkin, J. Am. Chem. Soc. 122 (2000) 12651.
[118] L. Cronin, P.H. Walton, Chem. Commun. (2003) 1572.
[119] S.J. Archibald, S.P. Foxon, J.D. Freeman, J.E. Hobson, R.N. Perutz, P.H. Walton, J. Chem. Soc., Dalton Trans. (2002) 2797.
[120] K. Weis, H. Vahrenkamp, Eur. J. Inorg. Chem. (1998) 271.
[121] C. Bergquist, G. Parkin, J. Am. Chem. Soc. 121 (1999) 6322.
[122] B.S. Hammes, X. Luo, M.W. Carrano, C.J. Carrano, Inorg. Chim. Acta 341 (2002) 33.
[123] M.M. Ibrahim, C. Pérez Olmo, T. Tekeste, J. Seebacher, G. He, J.A. Maldonado Calvo, K. Böhmerle, G. Steinfeld, H. Brombacher, H. Vahrenkamp, Inorg. Chem. 45 (2006) 7493.
[124] L.M. Berreau, M.M. Makowska-Grzyska, A.M. Arif, Inorg. Chem. 40 (2001) 2212.
[125] M.M. Makowska-Grzyska, P.C. Jeppson, R.A. Allred, A.M. Arif, L.M. Berreau, Inorg. Chem. 41 (2002) 4872.
[126] L.M. Berreau, R.A. Allred, M.M. Makowska-Grzyska, A.M. Arif, Chem. Commun. (2000) 1423.
[127] D.K. Garner, S.B. Fitch, L.H. McAlexander, L.M. Bezold, A.M. Arif, L.M. Berreau, J. Am. Chem. Soc. 124 (2002) 9970.
[128] D.K. Garner, R.A. Allred, K.J. Tubbs, A.M. Arif, L.M. Berreau, Inorg. Chem. 41 (2002) 3533.
[129] J. Xia, Y.-B. Shi, Y. Zhang, Q. Miao, W.-X. Tang, Inorg. Chem. 42 (2003) 70.
[130] R.A. Allred, K. Doyle, A.M. Arif, L.M. Berreau, Inorg. Chem. 45 (2006) 4097.
[131] K.J. Tubbs, A. Fuller, B. Bennett, A. Arif, L.M. Berreau, Inorg. Chem. 42 (2003) 4790.
[132] K.J. Tubbs, A. Fuller, B. Bennett, A. Arif, M. Makowska-Grzyska, L.M. Berreau, Dalton Trans. (2003) 3111.
[133] K.J. Tubbs, E. Szajna, B. Bennett, J.A. Halfen, R.W. Watkins, A.M. Arif, L.M. Berreau, Dalton Trans. (2004) 2398.
[134] O. Sénèque, M.-N. Rager, M. Giorgi, O. Reinaud, J. Am. Chem. Soc. 123 (2001) 8442.
[135] O. Sénèque, M.-N. Rager, M. Giorgi, O. Reinaud, J. Am. Chem. Soc. 122 (2000) 6183.
[136] O. Sénèque, M. Giorgi, O. Reinaud, Chem. Commun. (2001) 984.
[137] O. Sénèque, M. Giorgi, O. Reinaud, Supramol. Chem. 15 (2003) 573.
[138] O. Sénèque, M.-N. Rager, M. Giorgi, T. Prangé, A. Thomas, O. Reinaud, J. Am. Chem. Soc. 127 (2005) 14833.
[139] L.K. Thompson, B.S. Ramaswamy, E.A. Seymour, Can. J. Chem. 55 (1977) 878.
[140] B. Kaptein, L. Wang-Griffin, G. Barf, R.M. Kellogg, J. Chem. Soc. Chem. Commun. (1987) 1457.
[141] B. Kaptein, G. Barf, R.M. Kellogg, F. Van Bolhuis, J. Org. Chem. 55 (1990) 1890.
[142] R.M. Kellogg, R.P. Hof, J. Chem. Soc., Perkin Trans. 1 (1996) 1651.
[143] B. Koning, R. Hulst, A. Bouter, J. Buter, A. Meetsma, R.M. Kellogg, Chem. Commun. (1997) 1065.
[144] R.M. Kellogg, Phosph. Sulf. Silicon 120–121 (1997) 61.
[145] J.K. Voo, C.D. Incarvito, G.P.A. Yap, A.L. Rheingold, C.G. Riordan, Polyhedron 23 (2004) 405.
[146] J.T. Hoffman, C.J. Carrano, Inorg. Chim. Acta 359 (2006) 1248.
[147] S.C. Shoner, K.J. Humphreys, D. Barnhart, J.A. Kovacs, Inorg. Chem. 34 (1995) 5933.
[148] U. Brand, H. Vahrenkamp, Z. Anorg. Allg. Chem. 622 (1996) 213.
[149] C. Sudbrake, H. Vahrenkamp, Z. Anorg. Allg. Chem. 627 (2001) 857.
[150] C. Sudbrake, H. Vahrenkamp, Eur. J. Inorg. Chem. (2001) 751.
[151] F. Ekkehardt Hahn, C. Ochs, T. Lügger, R. Fröhlich, Inorg. Chem. 43 (2004) 6101.
[152] Müller, M. Ruf, H. Vahrenkamp, Angew. Chem. 106 (1994) 2164.
[153] B. Müller, H. Vahrenkamp, Eur. J. Inorg. Chem. (1999) 117.
[154] B. Müller, H. Vahrenkamp, Eur. J. Inorg. Chem. (1999) 129.
[155] B. Müller, H. Vahrenkamp, Eur. J. Inorg. Chem. (1999) 137.
[156] R. Vogler, M. Gelinsky, L.F. Guo, H. Vahrenkamp, Inorg. Chim. Acta 339 (2002) 1.
[157] M. Gelinsky, R. Vogler, H. Vahrenkamp, Inorg. Chem. 41 (2002) 2560.
[158] T. Bergman, K. Zhang, C. Palmberg, H. Jörnvall, D.S. Auld, Cell. Mol. Life Sci. 65 (2008) 4019.
[159] R.M. Kellogg, Pure Appl. Chem. 64 (1992) 413.
[160] D.J. Creighton, D.S. Sigman, J. Am. Chem. Soc. 93 (1971) 6314.
[161] D.J. Creighton, J. Hajdu, D.S. Sigman, J. Am. Chem. Soc. 98 (1976) 4619.
[162] R.A. Gase, U.K. Pandit, J. Am. Chem. Soc. 101 (1979) 7059.
[163] R.A. Hood, R.H. Prince, J. Chem. Soc. Chem. Commun. (1979) 163.
[164] A. Ohno, T. Kimura, H. Yamamoto, S.G. Kim, S. Oka, Y. Onishi, Bull. Chem. Soc. Jpn. 50 (1977) 1535.
[165] H. Awano, K. Takemoto, H. Ohya, M. Tomio, S. Tamagaki, W. Tagaki, Bull. Chem. Soc. Jpn. 60 (1987) 1887.
[166] A. Ohno, S. Oda, N. Yamazaki, Tetrahedron Lett. 40 (1999) 4577.
[167] S. Fukuzumi, N. Nishizawa, T. Tanaka, Chem. Lett. (1983) 1755.
[168] S. Fukuzumi, S. Koumitsu, K. Hironaka, T. Tanaka, J. Am. Chem. Soc. 109 (1987) 305.
[169] A. Kobayashi, H. Konno, K. Sakamoto, A. Sekine, Y. Ohashi, M. Iida, O. Ishitani, Chem. Eur. J. 11 (2005) 4219.
[170] K.I. Bäcklin, Acta Chem. Scand. 12 (1958) 1279.
[171] K. Burton, Biochem. J. 143 (1974) 365.
[172] L.E. Overman, J. Org. Chem. 37 (1972) 4214.
[173] E. Kimura, M. Sbionoya, A. Hoshino, T. Ikeda, Y. Yamada, J. Am. Chem. Soc. 114 (1992) 10134.
[174] E. Kimura, T. Shiota, T. Koike, M. Shiro, M. Kodama, J. Am. Chem. Soc. 112 (1990) 5805.
[175] R. Walz, H. Vahrenkamp, Inorg. Chim. Acta 314 (2001) 58.
[176] Y.H. Zhang, H. Vahrenkamp, Inorg. Chim. Acta 351 (2003) 201.
[177] C. Bergquist, L. Koutcher, A.L. Vaught, G. Parkin, Inorg. Chem. 41 (2002) 3533.
[178] B.V. Plapp, B.R. Savarimuthu, S. Ramaswamy, to be published, RCSB PDB entry 1YE3.